



POLITECNICO DI TORINO

Master of Science program in Energy and Nuclear Engineering

MASTER'S DEGREE THESIS

Scaling up Renewable Hydrogen in Ireland: Feasibility Study of a Hydrogen Production Plant for an Industrial User

Supervisors

Candidate

Pierluigi Leone

Francesca Catelan

Rory Monaghan

Co-supervisor

Marco Cavana

Acknowledgements

I would like to express my heartfelt appreciation to everyone who provided guidance and support throughout my Master's journey. Your contribution was essential to the success of this project.

First and foremost, I would like to express my sincere gratitude to my supervisors at Politecnico di Torino, Prof. Pierluigi Leone and Dr. Marco Cavana. Your support made it possible for me to pursue a part of this experience in Ireland, and your guidance and expertise were invaluable in ensuring its successful completion.

I am also deeply thankful to Prof. Rory Monaghan, Director of the Energy Systems Engineering Programme at NUI Galway. Your knowledge, insights, and advice have been essential in shaping and advancing this project.

I would also like to sincerely thank the entire Erin Research Group team. My appreciation goes to Fatemeh, Arjun, Thuso, Ahmad, and Haresh for generously sharing your time and expertise in your respective areas of research. Your feedback throughout the various stages of this project have greatly contributed to the development of my knowledge and skills in the hydrogen sector.

Finally, I would like to express my deepest gratitude to my family and friends for their constant support, encouragement, and love. I am especially thankful to my fiancé, Filadelfio, my greatest supporter, who stood by me through both the highs and the lows. To my parents, who always wished the very best for me, I owe endless thanks. I also want to acknowledge my nephews, Martino and Jacopo, because through your eyes, every possibility shines brighter. I hope the future brings you everything you dream of and more.

Abstract

Reaching net-zero emissions by 2050 will require the deployment of hydrogen as a central low-carbon energy vector. Despite its potential, the current green hydrogen value chain is still at an early stage, with only a small number of projects in operation worldwide.

In this context, the establishment of hydrogen valleys, combined with Ireland's abundant wind resources, could enable large-scale production of hydrogen, while playing a decisive role in helping reduce emissions for hard-to-abate sectors, such as heavy industry, transport, and power generation.

The decarbonization of energy-intensive industries represents a major challenge for meeting European climate targets. In particular, the cement sector is among the largest industrial emitters, and innovative solutions are required to reduce its carbon footprint. This thesis investigates the feasibility of integrating renewable hydrogen into an Irish cement production facility. The study initially considers three hydrogen integration pathways:

- The use of hydrogen in the cement production process
- The use of hydrogen for the transport fleet
- The combination of hydrogen with carbon capture and utilization (CCU) to produce e-fuels, specifically methanol.

After a preliminary assessment, only the transport application was deemed technically and economically viable, as the other two options were limited by regulatory gaps or prohibitive equipment and investment requirements.

The research then focuses on the design of a local renewable hydrogen production plant to supply the fleet. An hourly simulation model was developed in Excel and translated into Python to evaluate plant operation, renewable electricity supply, and hydrogen output.

A techno-economic assessment was performed, covering investment costs (CAPEX), operation and maintenance costs (OPEX), levelized cost of hydrogen (LCOH), and levelized cost of energy (LCOE). Sensitivity analyses were conducted to explore alternative implementation scenarios, including grid connection.

Results show that the proposed configurations can meet the company's transport demand both with an off-grid configuration and with a grid-connected supply in compliance with European Renewable Energy Directive III, altough grid contribution cannot be extensively exploited due to emissions contraints. The techno-economic assessment indicates that the cost structure is still heavily influenced by capital expenditure and the current market price of hydrogen-related technologies, which remain high compared to conventional transport fuels such as diesel. Nevertheless, ongoing improvements in electrolyzer efficiency and the expected scale-up of the hydrogen sector are projected to significantly lower costs in the coming years.

The design proves to be highly dependent on renewable availbaility and variability becomes the main challenge to overcome, especially linked to wind energy. The storage contribution helps mitigating variability but is not sufficient to fully eliminate it. The proposed configurations achieves an LCOH between 8.52 and $8.78 \in /kg$, depending on the selected configuration among the two proposed.

Beyond the specific case study, this work demonstrates the potential of hydrogen-based solutions for industrial transport and contributes to the broader scaling up of the hydrogen market.

Contents

1	Intr	roduction	13
	1.1	Green Hydrogen Production	14
	1.2	Hydrogen Storage	16
	1.3	Levelized Cost of Hydrogen	17
	1.4	Renewable Energy Directive III	18
	1.5	Hydrogen Valley's initiative	20
	1.6	SH2AMROCK: Ireland's Emerald Hydrogen Valley	22
	1.7	Aims, Objective and Novelty	23
	1.8	Thesis outline	24
2	Cen	nent Production Plant: Mannok case study	26
	2.1	Location	28
	2.2	Manufacturing process and energy requirements	30
	2.3	Cement emission profile	32
3	Hyo	drogen integration scenarios	35
	3.1	Literature review	36
	3.2	Production Process	42

CONTENTS

	3.3	Carbon capture and utilization: production of sustainable methanol	43
	3.4	Transport fleet	45
4	H_2	production plant model	48
	4.1	Power Farm	49
	4.2	Battery	49
	4.3	Electrolyzer	52
	4.4	Buffer, compressors and storages	53
	4.5	Grid connection	56
	4.6	Model corrections	57
	4.7	Refuelling profile	58
	4.8	Reduction of CO_2 eq emissions	61
	4.9	Python implementation	62
		4.9.1 Electrolyzer	63
		4.9.2 Renewable Farms	67
		4.9.3 Battery	67
		4.9.4 Compressor	69
		4.9.5 Storage	69
		4.9.6 Plant model	70
5	Plai	nt base-case design and techno economic assessment	72
	5.1	Cost analysis	72
		5.1.1 Renewable power farm	73
		5.1.2 Battery	74

CONTENTS

8	Con	clusion	1															104
7	Fut	ure woı	rk															102
	6.2	Optima	al desi	gn .				• •	 	•		 •	•	 •	•	 •		98
	6.1	Optima	al inve	stmen	t			• •	 		 •	 •		•			•	93
6	Sen	sitivity	anal	ysis														93
	5.4	Base-ca	ase de	sign di	scuss	sion .			 			 •		 •		 •		89
	5.3	Base-ca	ase pla	ınt des	sign				 							 •		79
	5.2	Leveliz	zed cos	t of er	nergy	/hyd	roger	1.	 							 •		77
		5.1.5	Stora	ge .					 	•		 •	•	 •				77
		5.1.4	Comp	ressor					 									75
		5.1.3	Electr	olyzer	٠				 								•	75

List of Figures

1.1	Characteristics of Hydrogen Valleys [9]	21
1.2	Localization of Hydrogen Valleys [9]	21
2.1	Location of Mannok cement plant	29
2.2	Mannok cement production process	30
3.1	Hydrogen integration scenarios	36
3.2	Cost projection of electrolyzer by emission reduction [43] [44]	46
4.1	Effective power by overall consumption	64
4.2	Production by overall consumption	65
4.3	Effective power by production	65
4.4	Overall consumption by effective power	66
4.5	Renewable farms class diagram	68
4.6	Plant model sequence diagram	70
5.1	Base case design methodology	80
5.2	Electrolyzer efficiency with respect to production rate (load)	81
5.3	H_2 production with respect to solar share, fixed capacity	82

LIST OF FIGURES

5.4	Battery size versus LCOH	84
5.5	Buffer size versus missing	86
5.6	HP storage size versus missing	87
5.7	MP-HP storage size combinations versus missing	87
5.8	HP storage size versus LCOH	88
5.9	Wind energy production	90
5.10	Buffer state of charge	91
5.11	Buffer curtailment	91
5.12	High pressure storage state of charge	91
6.1	Scatter plot on different configurations	95
6.2	LCOH by CAPEX	95
6.3	LCOH by CAPEX	96
6.4	Selected configurations	96
6.5	Optimal configuration comparison	97
6.6	Grid ON Configurations	99
6.7	Grid OFF Configurations	99

List of Tables

2.1	Mannok data overview and assumptions	32
3.1	Assumption for coal replacement	42
3.2	Hydrogen demand and preliminary design for coal substitution	42
3.3	CCU design assumption	44
3.4	Hydrogen demand estimation for methanol synthesis	45
3.5	Assumptions for fleet H_2 demand	47
3.6	Hydrogen demand estimation for transport fleet	47
4.1	Battery input parameters	50
4.2	Battery model	52
4.3	Buffer and storages parameters	54
4.4	Compressor's parameters	56
4.5	FCET characteristic	58
4.6	Dispenser characteristics and refuel frequency estimation	59
4.7	Reference day hourly H_2 consumption	60
4.8	H_2 emissions	62
5.1	PV Cost analysis-assumptions	73

LIST OF TABLES

5.2	Wind cost analysis assumptions	74
5.3	Battery cost analysis assumptions	75
5.4	Electrolyzer cost analysis assumptions	76
5.5	Available costs quotation for compressor	76
5.6	Compressor cost analysis assumptions	76
5.7	Storage reference specific cost	77
5.8	Hydrogen Refueling Station	77
5.9	Other investment parameters	78
5.10	Other parameters	79
5.11	Eletrolyzer cost analysis results	82
5.12	Wind farm cost analysis results	83
5.13	Battery cost analysis results	85
5.14	Buffer cost analysis results	85
5.15	Base-case plant design	88
5.16	Compressor cost analysis results	89
5.17	Economic key performance indicators	89
6.1	Optimal configurations	98
6.2	Overall results (buffer scaling)	100
6.3	key performance indicators (buffer scaling)	100
6.4	Overall results (HP scaling)	101
6.5	key performance indicators (HP scaling)	101
8.1	Kev parameters-base case	105

Nomenclature

AWE Alkalyne Water Electrolyzer

BAT Best Available Technology

BOP Balance Of Plant

CAPEX Capital Expenditure

CCS Carbon Capture and Storage

CCU Carbon Capture and Utilization

CCUS Carbon Capture and Utilization/Storage

CHP Combined Heat and Power

CMI Cement Manufacturers Ireland

DoD Depth of Discharge

EPA Environmental Protection Agency

EPR Environmental Performance Reporting

ETS Emission Trading System

EU European Union

FCET Fuel Cell Electric Vehicle

GHG GreenHouse Gases

NOMENCLATURE

HP High Pressure

HRS Hydrogen Refueling Station

IEA International Energy Agency

KPI Key Performance Indicator

LCOE Levelized Cost of Energy

LCOH Levelized Cost of Hydrogen

LOHC Liquid Organic Hydrogen Carriers

MP Medium Pressure

NPV Net Present Value

NZE Net Zero Emission

OPEX Operational Expenditure

PEM Proton Exchange Electrolyzer

PPA Power Purchase Agreement

PV photovoltaic

RED III Renewable Energy Directive III

RFNBO Renewable Fuel of Non Biological Origin

SAF Sustainable Aviation Fuel

SOC State Of Charge

SRF Solid Recycled Fuel

TCO Total Cost of Ownership

UF Utilization Factor

WACC Weighted Average Cost of Capital

1 Introduction

In 2015, the Paris Agreement highlighted the importance of staying below a 1.5°C increase in temperature to avoid permanent damage to the planet's well-being. Nevertheless, energy related CO_2 emissions reached a new record high of 37.4 Gt in 2023, increasing by 1.1% [1]. By analyzing the last decade from 2023, on the other hand, it can be noted that the rate at which emissions increase is significantly lower compared with a broader historical context and with global economic growth (evaluated though Gross Domestic Product). In fact, it is estimated an increase of about 0.5% per year. Clean energy can be addressed as the reason for this slowdown and is undoubtedly having an impact on the trend of CO_2 emissions.

By looking more closely at the European Union case, the growth of clean energy technologies accounted for half the decline in emissions and, as such, can be considered the most important driver. For the first time, wind power surpassed both natural gas and coal in electricity generation, favored by the northern region easier access to offshore wind resource, marking an historic milestone for the energy transition. Electricity production from coal dropped by 27% in 2023, while natural gas-based electricity generation declined by 15%[1].

Climate crisis is, by now, one of the big challenges of the historical period and Europe has been trying to track the trend of emissions and implement new strategies to support local nation actions towards reaching Net Zero Emissions and carbon neutrality.

In this context, green hydrogen presents itself as an energy carrier that shows huge potential in the decarbonization of energy, transport and industrial sectors, particularly for hard-to-abate ones. Although hydrogen presents many drawbacks compared to carbon sources, like higher volatility or lower gravimetric density, it does represent a feasible opportunity to avoid emissions related to certain activities, while both possibly exploiting existent technologies, like the gas network and creating a brand-new market to link economic growth with sustainability goals.

Hydrogen demand is still limited to refineries and industry applications, but in 2023, globally, it's possible to see a growth in new applications such as long distant transportation and heavy industry, even though it still accounts for less than 1% of global demand [2]. This expansion and integration trend is being supported by governments actions and policies that open the road to the economic growth of this new market.

On the production side, in 2023, 97 Mt of hydrogen were produced, but, based on announced projects, low-emissions hydrogen could reach 49 Mtpa by 2030 [2]. Hydrogen production is still largely dependent on fossil fuels, mainly on water gas shift reactions to convert natural gas. However, many new low emission production projects are being assessed through feasibility studies or reached final investment decision (FID). Most of these, about 55%, are based on electrolysis. For comparison, in 2023 the electrolizer's installed capacity was only 1.4 GW, but, through these projects, could reach 5 GW by 2030. The remaining 45% will be from fossil fuels with CCUS [2].

1.1 Green Hydrogen Production

As renewable technologies become more and more attractive and cost competitive, especially PV systems and wind farm, the interest in water electrolysis to produce green hydrogen grows too.

Today, there are three main technologies used in water electrolysis: Alkaline electrolyzers, Proton Exchange Membrane (PEM) electrolyzers and Solide Oxide electrolyzers.

Alkaline electrolyzers are mature and commercial technologies. They operate at low temperatures, between 60°C and 90°C and the electrolyte is a liquid, usually potassium

hydroxide KOH or sodium hydroxide NaOH[3]. Due to the absence of precious maters, particularly in the electrolyte, this is the less expensive technology. Unfortunately, it is also the less efficient one, with specific consumption between 50-78 kWh/kg [3]. This figure represents the consumption of electricity over the amount of hydrogen produced and is useful in representing and comparing the efficiency of the technology. Finally, the electrolyzer can operate at partial load with a lower limit of 15% and an upper of 100%, so it doesn't represent the most flexible option.

PEM electrolyzers present some similarities with alkaline ones. Particularly, the technology is commercially available, operates at low temperatures too, between 50°C and 80°C and contemplates the possibility of operating under high pressure, which is a particularly interesting option due to decreased costs of compression, kinetic enhancement of the process itself and higher efficiencies. The electrolyte consists of a solid material named Nafion, an acid polymer. The capital cost is higher compared to alkaline electrolyzers and the specific consumption is similar, between 50 and 83 kWh/kg [3]. PEM electrolyzers allows operation between 0-130% of the load, presenting higher flexibility Solid Oxides electrolyzers are still in the demonstration phase but seem to have huge potential. The electrolyzer works at high temperatures, between 650°C and 900°C and the electrolyte is a solid made of yttria-stabilized zirconia. Due to the high temperatures needed, it is highly expensive because the materials need to withstand thermal stress. However, the specific consumption is reduced to 40-50kWh/kg, allowing for less use of electricity, more efficiency and higher cost reductions in the stack lifetime [3]. For what concerns the load range, it is assessed between 20-125\%, representing a good compromise for flexibility. This technology needs to be further developed and will benefit from the economy of scale, once largely exploited, for diminishing the investment costs.

1.2 Hydrogen Storage

Hydrogen storage represents one of the many challenges of hydrogen integration, since hydrogen is a very volatile molecule and needs to be either compressed or liquified to be stored more easily and to increase the energy density.

Hydrogen is mostly stored in compressed tanks for stationary applications. Technology is mature even if it presents some issues, like safety. The compression is done from ambient conditions up to 350-700 bar and it consumes around 15% of the energy content of the fuel. At the end, the energy density is around 57.47 kg/m^3 [4] [5].

However, for large-scale projects, the most interesting option is represented by geological storage sites, like salt caverns. They retain low costs and high efficiency, meaning that almost all the hydrogen that is injected can, later, be recovered. Furthermore, salt caverns have very low risk of contaminating the hydrogen, which can, in this way, maintain its purity level.

Liquid storage is another option, and it requires hydrogen condensation below -253°C. The liquefaction consumes about 30% of the energy contained in the gas but allows to obtain a density of 71 kg/m^3 . Nevertheless, daily evaporation losses of 1-3% are to be considered and together with the high cost of liquefaction they still represent an issue for the use of the process. Still, it's interesting for aerospace applications and ship transport.

Considering material-based storage, metal hydrates and liquid organic hydrogen carriers (LOCH) are the most interesting options. The first one exploits a solid matrix, while the second a liquid one. Metal hydrates undergo an adsorption/desorption process governed by temperature changes: adsorption is exothermic, while desorption is endothermic. This reaches high energy density of about $150 \ kg/m^3$, it's intrinsically safe compared to other methods and can be done in wide pressure and temperature ranges [4]. The cost and life cycle assessment of the materials represents an issue and still must be further researched. The process is similar for LOHC: the concept is based on reversible exothermic hydrogenation and endothermic de-hydrogenation of carbon bounds. This solution presents

some advantages like offering long-term storage capacity without suffering leakage and boil-off; compatibility with the existing infrastructure for liquid fuels; release of high purity hydrogen; safe, cost effective and non-toxic technology.

1.3 Levelized Cost of Hydrogen

Hydrogen production methods are usually identified by color, making it easy to identify the production process and environmental impact related.

With the term green hydrogen, we refer to hydrogen which has been produced from water electrolysis. This process involves water splitting into hydrogen and oxygen through a flow of electric charges coming from renewable electricity plants. The process is considered as zero emission, and hydrogen subsequential use in heavy industry applications or transport allows to further reduce carbon dioxide emissions.

It is, however, characterized by high OPEX due to high amount of electricity needed and high dependency on electricity prices, and considerable CAPEX for the electrolyzer, even if, with more installations, the cost of the equipment is getting lower.

This is the main reason why green hydrogen is not yet widespread and used. It doesn't reach cost parity with other cheaper fuels, like grey hydrogen or diesel, and it represents a more expensive alternative, limiting its development and integration. To kickstart green hydrogen use, governments are implementing subsidies to levelize green hydrogen cost and policies that impose an increasing carbon tax, to incentivize the innovation in industries and the use of more efficient technologies, while increasing competitiveness of renewable technologies.

Levelized Cost of Hydrogen is the main figure used to assess hydrogen feasibility in its applications, and it varies based on technology considered, energy cost considerations and storage techniques or transport ones. This highlights the complexity of assessing LCOH and the variability of it. It is defined as the discounted lifetime cost of building and operating a production asset. It represents the total costs of a plant relative to the

hydrogen it is expected to generate over its lifetime, with both values adjusted to their net present value. It includes all relevant costs, investment and maintenance ones, taxes, electricity prices variations and it's expressed as cost per unit of hydrogen produced (\leqslant/kg) .

1.4 Renewable Energy Directive III

Adopted on 20 November 2023, the Renewable Energy Directive (EU) 2023/2413, RED III, reshapes the European Union's renewable energy framework. Whereas the 2019 directive required renewables to account for 32% of final energy consumption by 2030, the new legislation raises the level of ambition. The binding target is now set at 42.5%, with a further non-compulsory objective of 45%. This revision is closely aligned with the objectives of the "Fit for 55" package, designed to secure a 55% cut in greenhouse gas emissions by 2030. [6]

Different revisions and targets have been introduced for the various sectors. In the case of transport, for example, the directive provides a detailed set of criteria for the deployment of production plants for Renewable Fuels of Non-Biological Origin. Renewable hydrogen is included in this category, and its production facilities supplied with renewable electricity from the grid can be classified as 100% renewable, provided that the following conditions are met:

1. Additionality:

Electricity used for hydrogen production must come from new renewable capacity, not from plants that were already in operation, so that hydrogen demand stimulates extra generation rather than diverting existing supply. Specifically:

- (a) The renewable installation must be commissioned no more than three years before the electrolyser starts operating.
- (b) An energy asset under a Power Purchase Agreement is deemed operational concurrently with the electrolyzer's commissioning. Subsequent expansions of

that electrolyzer are permissible, provided they remain on the same site and are finalized within three years of the initial unit's start of operation.

(c) Renewable plants benefiting from financial support are excluded, with exceptions for repowering, or research/demo projects.

Derogation: until 1 January 2038, electrolysers commissioned before 1 January 2028 may use power from pre-existing renewable plants.[7]

2. Simultaneity:

To avoid stressing the power grid, renewable generation and hydrogen production must occur at the same time:

- (a) In the same hour when the renewable plant under PPA is generating; or
- (b) Using electricity stored behind the electrolyser's connection point, provided the storage was charged during that same hour; or
- (c) During hours when the day-ahead market clearing price is ≤ 20 €/MWh or lower than 0.36 of the ETS allowance price.

Derogation: until the end of 2029, monthly rather than hourly correlation is accepted. [7]

3. Spatial Correlation:

Hydrogen production, linked to renewable electricity plants, mustn't produce an excess of electricity for the grid or of installed capacity, to avoid congestion.

- (a) The renewable plant must be in the same bidding zone as the electrolyser; or
- (b) In a directly interconnected zone where day-ahead prices are equal to or higher than those of the electrolyser's zone; or
- (c) In an offshore bidding zone connected to the electrolyser's location.[7]

4. Greenhouse Gas Reduction:

Renewable hydrogen used in transport must achieve at least a 70% life cycle GHG reduction compared to fossil fuels (reference value: $94 \ gCO_2/MJ$). To compute the carbon footprint of electricity used:

- (a) If the electricity is fully renewable (as per Art. 27(3) of Directive 2018/2001), its emission factor is zero.
- (b) If not fully renewable, three calculation options apply: the first involves using the average GHG intensity for the respective Member State or bidding zone, assuming public data is accessible. Alternatively, if the electrolyzer's total operational hours remain below the time when renewable or nuclear sources set the marginal electricity price in the previous year, the grid electricity consumed is considered zero-emission. If exceeded, a default factor of $183\ gCO_2eq/MJ$ is applied. Finally, producers may opt to use the emission factor of the marginal generating unit at the moment of production, provided the data is reliably and publicly available.[8]

1.5 Hydrogen Valley's initiative

Among the European Commission's actions, there is the recent REPowerEU, a plan to phase out Russian fossil fuel imports, in response to the hardships and global energy market disruption caused by Russia's invasion of Ukraine. Implemented in March 2022, over the past years it helped achieve not only a reduction in gas consumption by 18% and the diversification of energy supplies for Europe, overcoming the dependency on Russian gas, but also an acceleration of energy transition by increasing the production of electricity from renewable energy sources. In this framework, Hydrogen Valleys have been identified as an essential implementation to scale up Europe's hydrogen economy.

Clean Hydrogen Partnership has been allocated a total of 215 M€funds by the European Commission to support 18 hydrogen valleys projects across 17 European countries[9]. The initiative brings together clean hydrogen production, storage and distribution to end-uses while creating regional value chains, all important characteristics that can be seen by a first glance in Figure 1.1.

The projects are divided by the amount of production between large-scale, with more

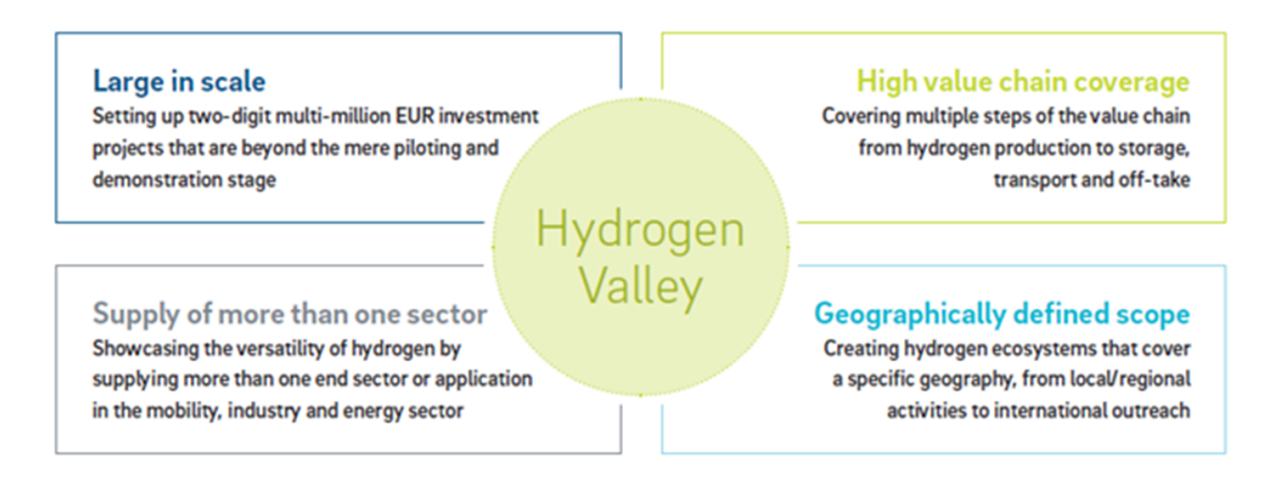


Figure 1.1: Characteristics of Hydrogen Valleys [9]

than 4000 t/year of H_2 produced and small scale, with a production of more than 500 t/year. Below is a geographical representation of the displacement and localization of the projects.

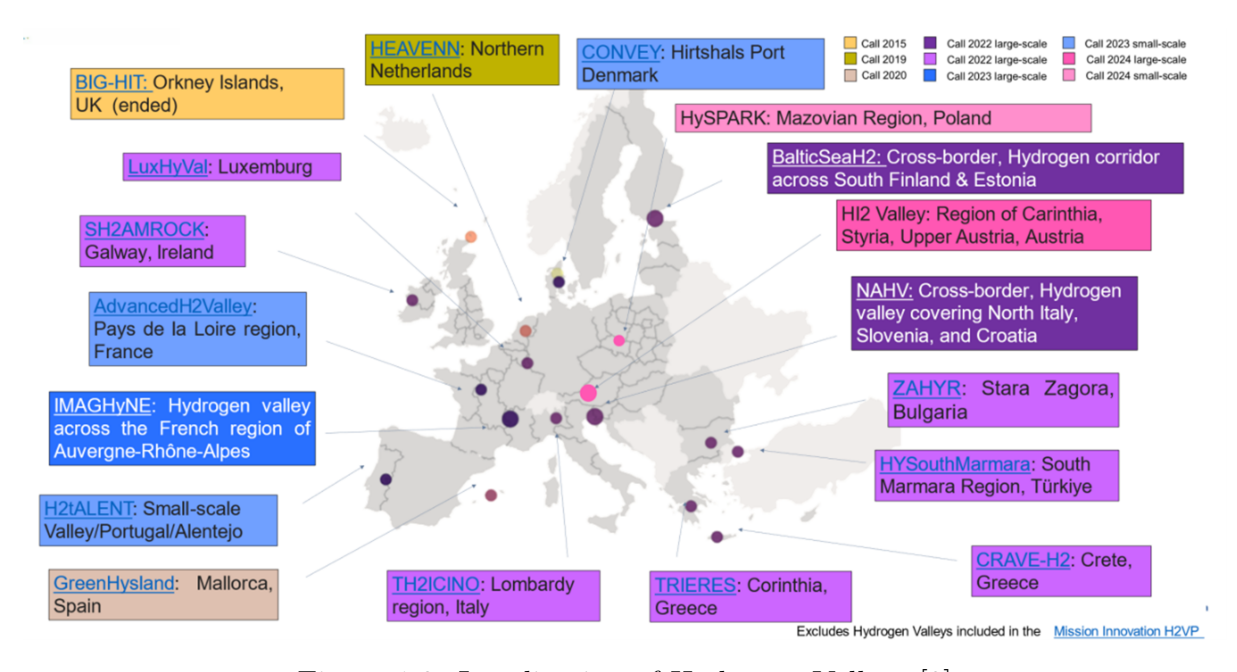


Figure 1.2: Localization of Hydrogen Valleys [9]

1.6 SH2AMROCK: Ireland's Emerald Hydrogen Valley

SH2AMROCK is a 5-year Irish project, supported by Clean Hydrogen Partnership and European Commission, with a total investment of approximately 80 M€, that aims at building and deploying Irish's first hydrogen valley [10].

This will bring major opportunities and change, with consequent challenges to create the know-how to manage the production and distribution, to analyze and renew the infrastructure, to create a domestic market for green hydrogen value chains. The project's logic is the exploitation of consistent wind resource, especially present in islands, to feed an electrolyzer and allow an isolated community to have more energy security, resilience and flexibility, to decarbonize multiple end-use applications through sector coupling and build stronger connections with other hydrogen valleys and economies in Europe.

The demand for hydrogen will also be profoundly changed by the decision to fund and develop this project. The project foresees a total electrolyser capacity of 4 MW, to be installed in two phases. The first 2 MW module, to be installed in Mount Lucas location, already authorised, will directly fill up to three tube trailers on-site. Electricity will be sourced both from the existing 84 MW wind farm located on site and from the grid. Hydrogen will be transported mainly using tube trailers to the different end-users. [11]

of vehicles in Galway. A 350-bar refuelling station will be developed to serve a wide range of vehicles, including double-decker buses, long-distance coaches, logistics trucks, delivery vans, minibuses, and maritime vessels. In addition, the port will host the Galway Centre of Excellence, dedicated to stationary fuel cell systems and pipeline-based hydrogen distribution. Combined Heat and Power (CHP) will also be installed at the port, for energy production and delivery.[11]

Industrial H₂ feeding is another end-use, used for industrial high temperature heating

systems to be installed at Colas plant, a local bitumen production plant. The site will be supplied by truck deliveries from the production facility.

At Connemara Airport, finally, hydrogen will support aviation testing activities, in particular flight trials of hydrogen-powered aircraft.

1.7 Aims, Objective and Novelty

This Master Thesis project aims to contribute to the scaling up of the Irish hydrogen consumption and market, through a feasibility study of a new renewable hydrogen production plant for industrial related use.

The selected industrial customer is a cement production facility located at the border between Northern Ireland and the Republic of Ireland. The facility is actively implementing sustainability measures and technological innovations to meet strict emission standards.

The study begins with an analysis of the energy needs of the cement plant and the development of possible hydrogen integration scenarios. Three main scenarios were considered:

- The use of hydrogen in the cement production process
- The use of hydrogen for the transport fleet
- The combination of hydrogen with CCU to produce e-fuels, specifically methanol.

After assessing these alternatives, two scenarios were found to be not feasible due to either the lack of regulatory frameworks, prohibitive equipment sizes, or excessive investment costs. Therefore, the study focuses on the design of a hydrogen production plant to meet the transport requirements of the company's fleet.

An hourly model was first implemented in Excel, including the main energy flows and components to simulate the plant operation in a year. The model was implemented in Python, to promote further research and facilitate the use of the hourly model and enable more advanced simulations.

Furthermore, a base-case design was evaluated, assuming fully renewable supply and assessing its economic feasibility through key parameters such as capex, LCOH, LCOE and opex. This base-case design helps to fix a reference, to be expanded and optimized in the sensitivity analysis.

To analyze the configurations representing optimal investments, in the sensitivity analysis a multi-objective optimization was carried out, through several model simulations.

Finally, an optimal design was presented, together with the analysis of all the design parameters and a focus on CO_{2eq} emission reductions, in compliance with the directives for renewable hydrogen.

1.8 Thesis outline

This thesis is structured into eight chapters:

• Chapter 1: **Introduction**

This chapter provides background information on hydrogen production and storage, as well as its levelized cost and the regulatory framework. It also presents ongoing hydrogen development projects promoted by the European Union. Finally, the motivations and structure of the thesis are explained.

• Chapter 2: Mannok case study

The chapter describes the selected industrial costumer, outlining its manufacturing process and its main energy and production figures.

• Chapter 3: Hydrogen integration scenarios

In this chapter, the possible hydrogen integration routes are introduced, namely in the production process, through carbon capture and utilization and in the transport fleet.

• Chapter 4: Hydrogen production plant model

This chapter provides a thorough explanation of the Excel model and its Python

implementation, describing its operating conditions, limitations and possible applications.

• Chapter 5: Plant base-case design and techno-economic assessment

In this chapter the base-case design will be presented, along with the cost analysis. The outcomes will be presented with a focus on key parameters such as LCOH, LCOE, Capex, Opex and the design will be used as reference case to pursue the optimization.

• Chapter 6: Sensitivity analysis

This chapter presents the sensitivity analysis, where a multi-objective optimization and a new optimal design will be presented, derived from many alternative plant design simulations and a thorough data analysis. For the optimal investments scenarios and for the optimal design the key parameters are presented and discussed.

• Chapter 7: Future work

This chapter suggests directions for further research, exploring alternative pathways for hydrogen integration within the facility.

• Chapter 8: Conclusions

The final chapter summarizes and discusses the main findings and outcomes of the thesis.

2 Cement Production Plant: Mannok case study

Cement is a hydraulic binder usually employed in concrete, to bind together fine sand and coarse aggregates. Concrete, in which cement is employed, is the second most used substance in the world, after water, with more than 4 billion tonnes of manufactured cement per year [12]. Its widespread nature makes it essential for construction and infrastructure development. However, the manufacturing process of cement is associated with high CO₂ emissions, making it responsible for about 7% of global CO₂ emissions [13]. This carbon dioxide is not only coming from combustion of fuels, which accounts for only 40% of it, but the biggest share is intrinsic to the process. In fact, about 60% is generated from the calcination reaction of limestone, the essential chemical reaction for clinker manufacturing [13].

$$CaCO_3(s) \longrightarrow CaCO(s) + CO_2(g)$$

The formation of calcium oxide (lime), main component of clinker, releases CO_2 which is denominated as process emission.

This combination of high environmental relevance and economic importance, together with widespread exploitation of this material, puts the cement sector at the forefront of the green, net-zero transition, especially within European climate neutrality policies.

Usually, cement manufacturing plants are characterized by huge production and energy

intensity, and this is often coupled with the widespread use of fossil fuels for delivering the needed thermal energy for the kiln and pre-heater. This is because coal and derivatives represent cheap and optimal fuels, especially due to their solid nature, which, through the kind of flame and burning properties, creates the right conditions for homogeneous temperature distribution and developing of the chemical reaction.

Nevertheless, many sustainable projects and actions are being implemented to decarbonize the sector, and much attention is being paid to the design of the right technologies to achieve this task.

Cement sector is considered a hard to abate sector. Some strategies to help decarbonize it consist mainly in increasing energy efficiency and thermal energy management through heat recovery, partially substituting fossil fuels with alternative fuels such as biomass or solid recovery fuel or changing the final clinker composition by reducing the share of clinker and increasing the share of supplementary cementitious material [13]. Nevertheless, the only way to fully decarbonize the process, due to its intrinsic CO_2 emissions, is through CCUS. Through this technology implementation, the CO₂ formed during the limestone decomposition reaction is captured and stored in underground reservoirs. This trapped CO₂, on the other hand, could become a revenue stream if used, together with renewable hydrogen, to produce e-fuels such as methanol or SAF. In principle the technologies are available to decarbonize the sector, but in practice the economic factor is limiting the actual installation or retrofitting. Infact, for the adoption of the boldest technologies, from a carbon neutral point of view, it is often necessary to do a radical re-design of the whole production plant. Most components must be switched out for new ones and there is a high investment cost, that makes it unfeasible to adopt these technologies.

In this framework, Mannok positions itself as a leader for sustainable transition. It is, in fact, admirable how the group is always looking for new strategies to reduce their carbon emission, from adopting best available technology and integrating innovation into their processes, to applying for European and UK funding schemes to integrate renewables into

their energy mix.

Mannok, formerly known as Quinn Group, with almost 50 years of heritage, deals with the production and sale of a wide variety of construction products, such as insulation, roof tiles, and cement. The company has grown, since 1970, becoming one of the most important players in the construction sector of UK and Ireland [14].

At the center of Mannok's operations is its advanced cement production facility in Derrylin, Northern Ireland. This site not only provides cement to supply the English and Irish demand but is also the precursor of other products of the company in the building sector, from precast concrete elements to roof tiles and structural systems.

Beyond construction, the industry has developed a significant presence in the packaging industry. Its packaging solutions, both rigid and flexible ones, allow the industry to supply different sectors, including agri-food, industrial manufacturing, and logistics.

In parallel, the company's insulation business is aligned with sustainability trends of energy efficiency commitment. Through the production of advanced PIR (polyisocyanurate) and EPS (expanded polystyrene) insulation panels, Mannok supports the transition toward more energy-efficient buildings and compliance with progressively stricter regulations.

2.1 Location

Mannok presence is spread between Northern Ireland, where its headquarters are located, and Republic of Ireland, where offices and facilities are set. Mannok Cement, the original cement production site, has been set up since 1989, in Derrylin, Co. Fermanagh. Nevertheless, a second cement production plant, Scotchtown Cement Works, was commissioned in 1998 in Ballyconell, Co. Cavan, due to an increase demand in construction products.

Its strategic location enables the company to supply both the UK and Republic of Ireland

markets. The main operational site is not only situated in a rural area adjacent to the quarry but also benefits from excellent transport links across the island, ensuring efficient movement of raw materials and swift distribution of finished products.

The site allows the future development of investments towards Net Zero and low carbon energy strategies, thanks to the wide industrial area available. In fact, since 2008, a wind farm, Slieve Rushen Repowering, has already been commissioned, featuring 54 000 kW of nominal power and 18 Vestas V90/3000 turbines [16].

The wind farm in question is often curtailed by the national grid and could be further exploited in the cement production plant.

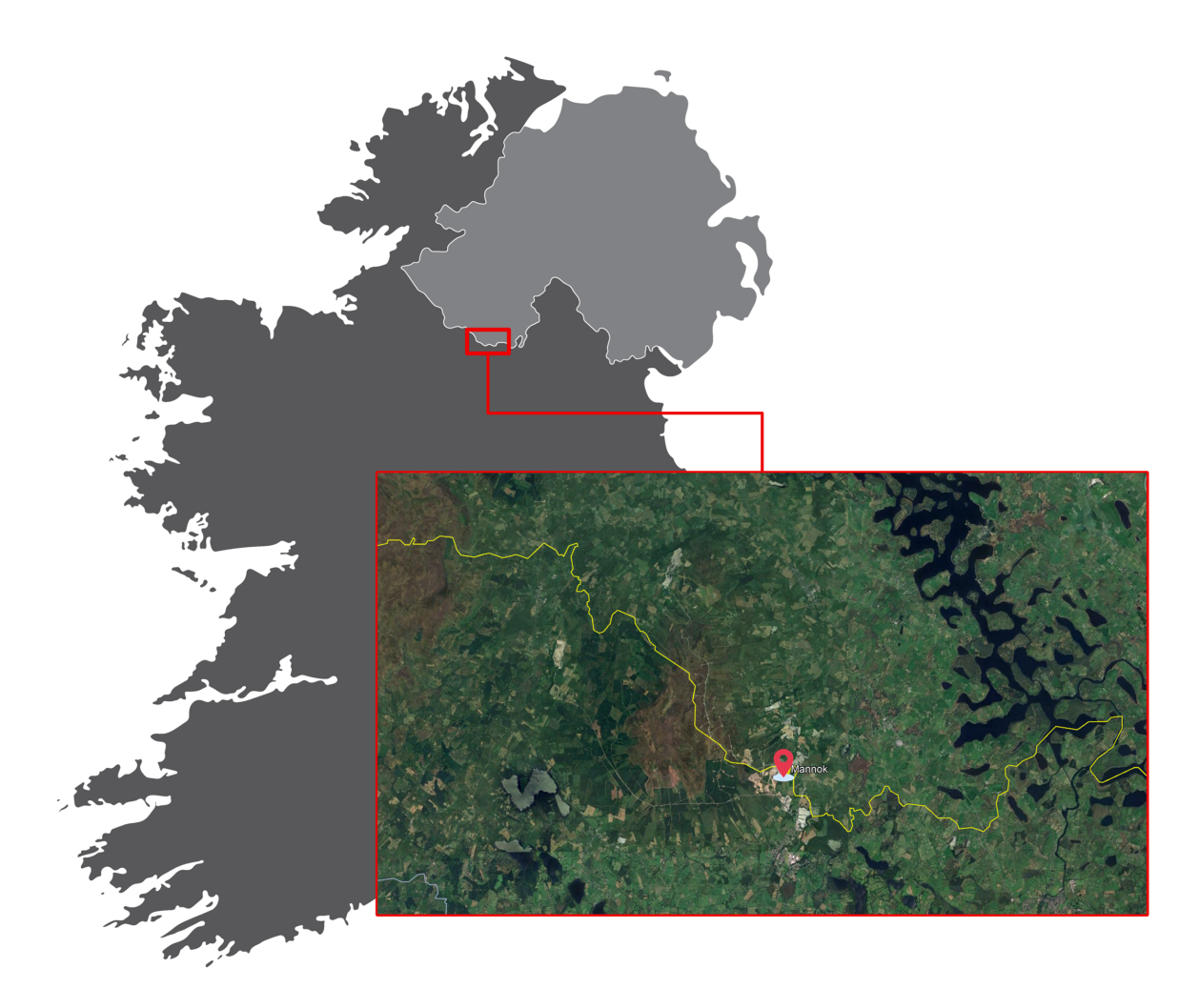


Figure 2.1: Location of Mannok cement plant

2.2 Manufacturing process and energy requirements

The final product of the facility is Portland Cement, composite of synthetic minerals and used to produce concrete.

The manufacturing process to produce Portland cement is subdivided in different stages.

Firstly, there is the extraction and pre-processing of raw materials, mainly limestone, shale and clay, that provide four fundamental elements: calcium oxide, silicon oxide, aluminum oxide and ferrous oxide. The materials undergo primary crushing and are, then, mixed with other components in controlled proportions, to form a uniform blend: the raw meal. This can be done either in wet processing, forming slurry, or in a dry one, through dry mixing.

In the pre-heater, the raw meal is heated to 800°C, through heat recovered from the exhaust of the calciner.

The main stages of the production process are the calcination, through the calciner, where 95% of the calcination happens and the product undergoes thermal decomposition at 900°C, and the sintering, trough the kiln, reaching a peak temperature of 1500°C and feeding further thermal decomposition, finally producing clinker. The clinker, made of silicates, aluminates and ferrites of calcium, coming from the oxidation of the same oxides is, then, rapidly cooled, to preserve the hydraulic properties[15].

The further mixing and crushing of clinker with additives and other substances gives the final product: Portland cement.

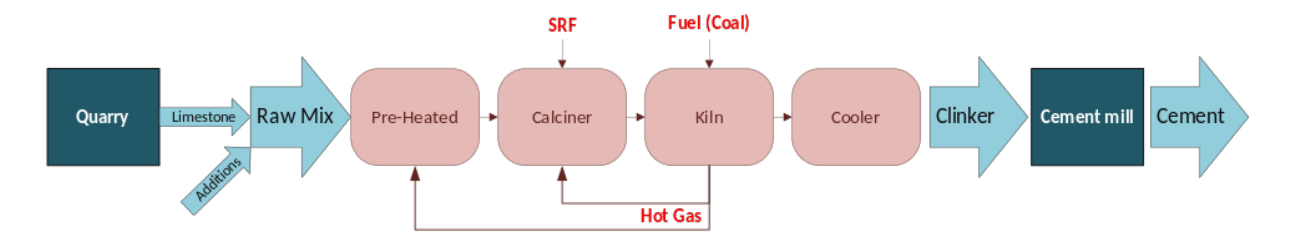


Figure 2.2: Mannok cement production process

The production of clinker is highly energy intensive, and the different sources of energy

needed are [17]:

- Thermal energy: about 80-90% of the energy needed for the entire process, corresponding to the need of the kiln system. Difficult to electrify and needs further technological improvement and fuel intervention.
- Electrical energy: power mills, conveyors, fans, pumping systems, compressors, filtration and environmental control systems.
- Water resource: needed mainly for cooldown purposes

The necessary thermal energy for the pre-heater, the calciner and the kiln usually comes from fossil fuels. Various fuels can be used, but the main fossil fuels used in Europe are coal and petroleum coke. They represent cheap and highly available sources of energy, which is an important requirement because cement production plants usually deal with significant flows of materials and cement and are highly energy intensive. Furthermore, the fuel doesn't have specific needs in terms of purity level or chemical characteristics, other than the lower heating value. An easily implemented improvement, which Mannok has employed as well, is the use of biomass or waste to substitute part of the coal. In Mannok case the choice has fallen to SRF, which provides about half of the thermal energy needed for the process, halving the amount of coal.

Theoretically, the thermal energy needed for the reaction of clinker is about 1700 MJ/ton of clinker [18], but realistically, since 2020, European cement plants consume around 3600 MJ/ton of clinker [19]. Electricity demand, on the other hand, has risen to nearly 100 kWh per ton of cement.

In the NZE scenario for 2030, gradual improvement are expected, with thermal intensity reducing to 3.4 GJ/t clinker and electricity use declining to 90 kWh/t cement. [19]

The specific thermal consumption of Mannok, derived from the company's fuel consumption and clinker production data, is consistent with the European average of 3,6 GJ/ton of clinker. This is due to the implementation of BAT in the process. The newest energy efficiency improvement was the adoption of FUELFLEX® Pyrolyzer, specifically

developed for the cement industry to replace all calciner fuel by SRF ensuring complete combustion, efficient NOx control and process stability. It is a new type of fluidized bed pyrolyzer, specifically developed to operate with extremely fine cement raw meal and it is employed together with the cement kiln. By using SRF in the calciner, the CO_2 emissions were cut by $58,000\ tCO_2eq$ in a year. [20] [21]

As confirmed by IEA, the adoption of low carbon fuels will be decisive in order to reduce the share of fossil fuels to 79% by 2030, in compliance with the NZE Scenario, which provides that the renewable energy waste should increase to 16% and hydrogen to 2% of total thermal energy share. [19]

This trend is being reinforced by the positive example led by Germany. Over the past three decades, the German cement industry has reported an average specific thermal energy demand of about 2850 MJ per tonne of cement. During this period, there has been a steady shift from fossil fuels towards alternative fuels such as waste wood, sewage sludge, and SRF. By 2020, these alternatives accounted for roughly 70% of the sector's total thermal energy demand. [22]

Mannok Data overview

Annual cement production	1.7	Mtons	[15]
Specific thermal consumption	3600	MJ/tons of clincker	[42]
Electricity consumption	100	kWh/tons of clinker	[42]
ETS allowances	561 366	$tCO_2eq/year$	[23]

Table 2.1: Mannok data overview and assumptions

2.3 Cement emission profile

Cement production plants could become, in the future, important hubs to the integration of renewable technologies and innovation. Thanks to the intensive use of energy, and consequently large amount of CO₂ emissions, the sector is continuously subjected to research and green hydrogen integration could be an innovative and economically attractive opportunity.

The new hydrogen valley in Galway will open the road to new hydrogen market and higher consumption of hydrogen will require more production of it.

To evaluate hydrogen implementation, an initial assessment of the cement plant's production and consumption characteristics was conducted. Through data provided by the facility, the process's thermal requirements, annual operating hours and load, as well as the associated CO₂ emissions were evaluated.

Mannok Cement takes part in the EU Emissions Trading Scheme (EU ETS), with its yearly greenhouse gas emissions independently verified and submitted to Ireland's Environmental Protection Agency (EPA) through the Climate Change Unit and the Environmental Performance Reporting (EPR) platform. As a member of Cement Manufacturers Ireland (CMI), the company follows the CEMBUREAU 2050 Carbon Neutrality Roadmap, which sets out the pathway to achieving net-zero emissions across the cement and concrete industry. Mannok Cement remains dedicated to lowering its environmental impact and contributing to the shift toward a carbon-neutral economy. [15]

In cement production, the kiln system represents the predominant source of atmospheric emissions. These emissions result from both the physical and chemical transformations of the raw meal and from the combustion of fuels within the process. The flue gas is primarily composed of nitrogen and residual oxygen from the combustion air, as well as carbon dioxide and water vapor generated from the decomposition of raw materials and the combustion process, which is inherently integrated into clinker production. Trace concentrations of regulated air pollutants are also present in the exhaust stream. According to the Best Available Techniques Reference document for the cement sector (European Commission, 2010), the main atmospheric pollutants associated with the process include [17]:

• Nitroge Oxide (NO_x) ;

- \bullet Sulphur Dioxide (SO₂) and other sulphur-containing compounds;
- Particulate matter (dust);
- Volatile organic compounds (VOCs)
- Polychlorinated dibenzo-p-dioxins (PCDDs) and dibenzofurans (PCDFs);
- Metals and their associated compounds;
- Hydrogen fluoride (HF);
- Hydrogen chloride (HCl);
- Carbon monoxide (CO);
- Ammonia (NH₃);

3 Hydrogen integration scenarios

Thus far, comprehensive hydrogen integration solutions for the cement industry have been carried out to explore the bottlenecks and the possibilities related to the decarbonization of this hard to abate sector.

Thorough examination has been conducted regarding the various technologies applicable to get the cement sector up to speed with the increasingly tight limits on the CO_2 emissions imposed by the ETS and European legislations.

More research needs to be conducted, but, as Ireland aims to become a reference point for hydrogen development and export, understanding the state of the art in hydrogen integration strategies and techno-economic scenarios for hydrogen implementation in cement plants becomes imperative.

Moreover, expanding hydrogen production and utilization and reinforcing hydrogen supply chain is a key step for the sector's development. Hydrogen integration is a possible road for many industrial applications.

In the case study, the evaluated scenarios are three:

- 1. Hydrogen integration in the manufacturing process
- 2. Hydrogen integration in the transport fleet
- 3. Hydrogen utilization with CO₂ from carbon capture for methanol production

The upstream plant configuration is kept the same for all three scenarios and it is composed of: power farm; battery storage; electrolyzer; hydrogen storage.

The end use, on the other hand, differs: in the first case, the hydrogen would be directly taken from the storage and used in the cement kiln and/or calciner. In the second case, an hydrogen refueling station needs to be installed and hydrogen would be used as fuel for the fleet. Finally, the third scenario implies a carbon capture system and another reactor plant to convert hydrogen and CO₂ into methanol.

The three scenarios are analyzed in terms of energy/fuel needed and preliminary design.

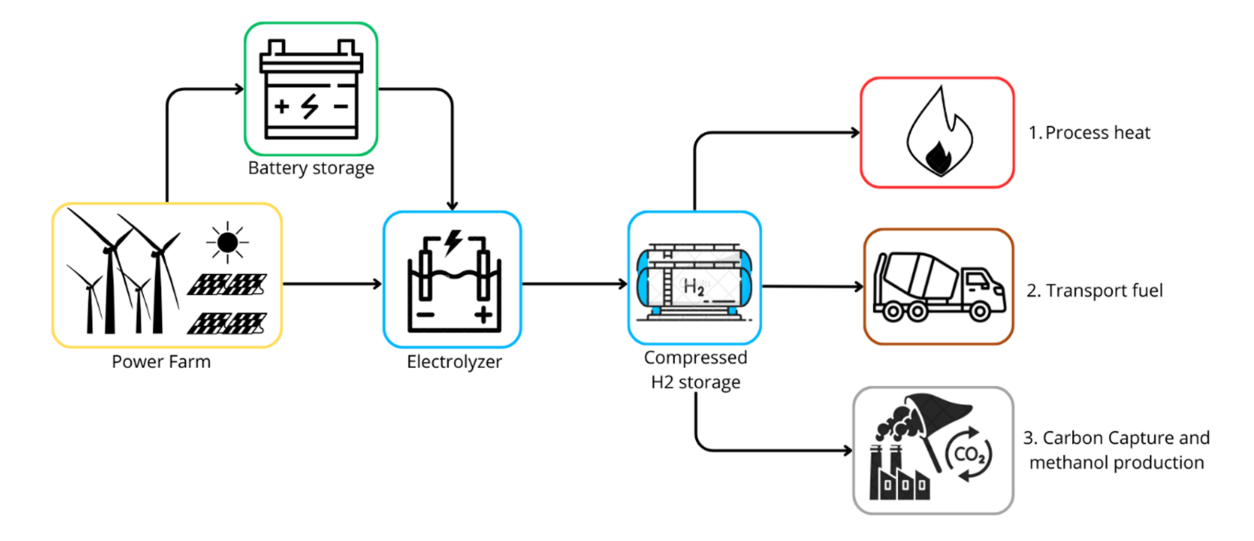


Figure 3.1: Hydrogen integration scenarios

3.1 Literature review

Williams et al. [25] provide valuable insights into possible decarbonization routes for clinker production by exploring the use of hydrogen as an alternative fuel and the integration of oxy-combustion with carbon capture systems. Using an Aspen Plus simulation, the authors examined six process setups for clinker manufacturing, each varying in fuel type, oxygen supply mode, and CO₂ capture approach, and compared their energy consumption and emission performance. Among the analyzed options, the oxyfuel process powered by natural gas emerged as the most energy-efficient, requiring roughly 35% less energy than the reference scenario, which relied on amine-based post-combustion CO₂ capture in a conventional natural gas-fired kiln. This finding highlights the strong potential of oxyfuel technology, whose efficiency gains outweigh the extra energy needs of

the air separation unit. In the hydrogen-based configurations, total energy demand decreased by 11% to 33% relative to the reference case. The lower savings mainly result from the energy losses associated with water electrolysis, which become more significant per ton of clinker as the hydrogen share rises. Nonetheless, advancements in electrolyser performance were shown to considerably mitigate the overall energy requirement of these hydrogen scenarios.

Desport et al.[26] investigated the possibility of achieving net-negative emissions in the cement sector through the integration of bioenergy and carbon capture and storage (BECSS). With 65% clinker-to-cement ratio becoming the standard and high penetration of biomass and CCS, the cement sector could even aid other hard-to-abate sectors, generating emission allowances.

Obrist et al.[27] examined a decarbonization pathway to pursue by 2025 for the Swiss cement industry. In this study, CCS becomes economically viable only when the carbon price exceeds 70€per tonne of CO₂.

Similarly, Kroumian et al.[28] explored the feasibility of achieving full fuel substitution with alternative fuels under oxyfuel conditions using a pilot-scale burner designed for retrofit applications in cement kilns. The experiments demonstrated stable combustion of SRF, wood, and sludge in both air and oxyfuel environments. Compared with coal, these alternative fuels produced longer and broader flames with a lower initial heat flux that stabilizes over time, whereas coal combustion have a shorter and more intense flame close to the burner. The study also highlighted the importance of recirculation rates in governing combustion dynamics: by tuning recirculation rate, it is possible to achieve combustion characteristics similar to air-fired operation while enhancing flame stability.

Decarbonizing the cement industry will require more than one strategy. Oxyfuel with CCS offers the highest efficiency gains, hydrogen provides additional potential, with electrolysis becoming more efficient, and fuel conversion to bio-based will be essential, even achieving 100% of utilization. Together, these strategies show that combining fuel substitution, CCS, and process optimization is essential to align the sector with net-zero targets.

Barigozzi et al. [29] investigated a systemic approach in the analysis of a hydrogen production plant for a case-study industrial user in Portugal. The findings involve an optimization procedure for both technical parameters and economic ones. Optimizing for cost versus efficiency results in different plant designs: when minimizing the LCOH, both electrolyzer and storage tank capacities are reduced by 30-50%. The production cost of green hydrogen ranges from about 10 USD/kg at a renewable fraction (RF) of 40% to 11.5 USD/kg at RF = 100%.

Ibáñez-Rioja et al.[30] evaluated baseload hydrogen supply from an off-grid PV-wind power generation unit based in Finland with battery storage, electrolyzer and hydrogen seasonal storage system based on salt and rock cavern geologies. An optimization of the system to minimize the LCOH was carried out, resulting in $2.77 \in /kg$ for salt cavern storage compared with $3.14 \in /kg$ for the rock cavern system, outlying the feasibility and competitiveness of an off-grid hydrogen production site.

Pilotti et al.[31] explored the use of seasonal storage for hydrogen, to be used for power-to-power applications in Sicily, to reduce dependency from mainland electricity. The round-trip efficiency of hydrogen storage results to be relatively low (22-27%), but the possibility of large-scale geological storage allow for higher capacity and reduced energy curtailment. Nevertheless, power-to-power hydrogen meets less than 5% of the total electricity demand.

The research mentioned above was useful in outlining key steps and processes of the hydrogen production plant design. Moreover, they provided a useful benchmark for comparison and assessment of the significance of the results obtained in this thesis. Overall, current research highlights both the technical feasibility and the economic challenges of hydrogen production plants. While significant progress has been made in system integration and cost reduction, further developments are required to ensure large-scale, competitive deployment.

Kunasegeran et al.[32] presented a thorough review of CCUS options for decarbonizing the cement industry. Absorption methods were analyzed first, showing that it is possible to capture 80-90% of CO₂, mainly by using Monoethanolamine (MEA), which is the most common chemical solvent. However, this approach has important drawbacks, primarily due to the high energy demand for solvent regeneration, since the water-based solution must be heated close to boiling to release the absorbed CO₂. Adsorption techniques were then considered. Their main advantage is the simpler regeneration of adsorbents, and they can achieve CO_2 recovery rates of 95-100%. Common adsorbents include activated carbon, zeolites, silica gel, and alumina. Another method discussed is Calcium Looping, which can capture around 93-94% of CO₂. This process is based on the exothermic reaction between CaO and CO₂ from flue gases at 600-700 °C, producing CaCO₃. The $CaCO_3$ is then sent to a second reactor (the calciner), where it is decomposed at > 900 °C (under oxy-fuel conditions), releasing pure CO₂ and regenerating CaO for reuse. Other CCUS technologies mentioned include Chemical Looping Combustion, Cryogenic Separation, and Membrane Separation, which are still mostly at the research stage. Finally, Oxy-fuel combustion was described as an indirect CO₂ capture approach. In this method, fuel is burned with pure O₂ instead of air, producing a flue gas that is already CO₂-rich due to the absence of nitrogen. However, in cement plants this method can only be applied in the pre-heater section, as the kiln combustion becomes unstable under pure O_2 . Therefore, only part of the total CO_2 emissions can be captured.

Barbhuiya et al. [33] proposed a roadmap to a net-zero carbon cement sector. The paper reviews emerging low-carbon technologies such as alkali-activated binders, calcium looping, electrification, and bio-inspired solutions. By considering the economic aspects and regulatory frameworks, it discusses challenges and possible solutions, outlining possible future directions.

Rafiq et al.[34] analyzes the CO₂ utilization for chemical production in the cement sector, from an environmental and economic point of view. This study investigates opportunities in Thailand's cement sector, exploring the conversion of captured CO₂ into urea, dimethyl ether (DME), and methanol. The analysis combines life cycle modeling with economic evaluations to assess feasibility under different policy scenarios. Within the different chemical pathways for CO₂ utilization, urea synthesis showed the greatest potential for

emission reduction, avoiding up to 3.47 kg of CO₂ for each kilogram processed. Profitability, however, is strongly dependent on electricity costs, with the process becoming competitive when prices drop below 20 USD/MWh.

This research provided a solid background on carbon capture and utilization methods in the cement sector and was thoroughly reviewed in the process of evaluating CO_2 capture and utilization methods for the present work.

Genovese et al. [35] presented an overview of the technological status on hydrogen refueling stations and research enhancement. Through data elaboration on hydrogen vehicles and sectors in the past years, recent publications and a synthesis of needs and requests of hydrogen applications, the author gave a comprehensive overview of comprehensive knowledge. In the paper, then, hydrogen refueling stations were examined in different layouts and combinations, considering geographical location and technology adopted for gaseous and liquid stations. The analysis concludes with a comparison that highlights the main advantages and drawbacks of each of them, emphasizing the limits imposed by the lack of the infrastructure needed for hydrogen refueling stations.

Gunawan et al. [36] presented a techno-econo-environmental modelling of various options to decarbonize fleets of four-axle trucks in the quarrying sector, considering total cost of carbon emission abatement as primary parameter, calculated from the total cost of ownership (TCO) and well-to-wheel (WTW) emissions. It is shown that on-grid systems enable optimal equipment sizing thanks to stable electricity supply, resulting in lower TCO and TCA. Off-grid configurations, instead, require oversizing to cover full fuel demand; otherwise, BETs and FCETs meet only 42% and 62% of their needs. Yet, despite higher costs, off-grid options achieve lower emissions due to the carbon intensity of grid electricity.

Kast et al.[37] investigates the design of medium and heavy-duty hydrogen fuel cell electric trucks, providing insight into the different categories of vehicles and their characteristics and analyzing the necessary amount of hydrogen storage for desired range, storage potential by tank location, and the maximum and minimum vehicle range estimates, for

both 350 bar and 700 bar storage pressures.

Martorelli et al.[38] analyzed hydrogen refueling process for heavy-duty vehicles according to the SAE J2601/2 protocols. Through a thermodynamic model implemented in a Matlab/Simulink environment, the refueling process of a 28 kg storage system of a heavy-duty vehicle is simulated, evaluating the storage system on board the vehicle as a multi-tank system and not as a single tank with an overall volume, as prescribed by the standard. The difference highlighted is the geometry, which influences convective heat transfer and brings to an overestimation of the temperature in the single storage configuration, which in turn impact the refueling time and flow. With multi-tank approach the paper evidences a time saving in refueling time of 5 to 10%, depending on the scenario considered. Furthermore, when the maximum peak flow rate was doubled across all scenarios, refueling time was reduced by more than 50%, while the increase in temperature and pressure remained within the limits allowed by the SAE protocol.

Oztürk et al.[39] investigated the optimal design and techno-economic performance of an on-site hydrogen refueling station powered by a hybrid wind and solar photovoltaic system in Turkey. The analysis shows that LCOH values in the HRS system range from 4.5 to $43.6 \in /kgH_2$, depending on the installed capacity of the renewable energy system and the project lifetime. Higher LCOH values are associated with short-term investments and low daily hydrogen production rates. The most cost-effective configuration is represented by a 5 MW PV farm and 400 kg of daily hydrogen demand, achieving an LCOH of 4.5 \in /kgH_2 in a 20-year long-term investment.

This thesis places a strong emphasis on hydrogen applications in the transport sector, a key focus of the project. The studies mentioned before not only contributed to sharing relevant knowledge but also provided valuable inputs, some of which were adopted as assumptions in the present work.

3.2 Production Process

The partial replacement of coal with hydrogen was assessed in order to estimate the plant's potential hydrogen demand. Through Mannok's data on annual cement output and coal consumption, the hydrogen requirement was estimated at around 13.1 Mtons per year. This figure comes from assuming a lower heating value of 29 MJ/kg for coal and 120 MJ/kg for hydrogen. To evaluate the nominal capacity of an electrolyzer able to meet the demand, an efficiency of 60% and 8260 operating hours per year were assumed, corresponding to an installed capacity of approximately 88 MW.

Assumptions

LHV coal	29	MJ/kg	[40]
LHV solid recycled fuel	15	MJ/kg	[40]
LHV hydrogen	120	MJ/kg	
Electrolyzer average efficiency	15	MJ/kg	[41]
Electrolyzer operating hours	8260	h/y	

Table 3.1: Assumption for coal replacement

Estimations

Estimated hydrogen demand	13100	t
Electrolyzer estimated size	88	MW

Table 3.2: Hydrogen demand and preliminary design for coal substitution

However, this scenario was not pursued further, as it would require substantial modifications of the existing plant, excessive costs and the availability of components sizes, such as the electrolyzer, that are not yet commercially available. Moreover, fuel substitution with hydrogen would only abate around 30% of total $\rm CO_2$ emissions, while the remaining 70% from calcination reactions would persist. For these reasons, large-scale coal substitution with hydrogen was excluded from the scope of this thesis.

Furthermore, based on the current state of research on hydrogen use in cement plants and IEA's outlook on future integration strategies, it is clear that complete or large-scale fuel substitution with hydrogen will not be a pursued road, nor is it expected to be a feasible option.

Another possible way to integrate hydrogen into clinker production concerns, for example, the UTIS patent, which introduces small amounts of H₂ into the combustion chamber. This approach enhances combustion completeness and efficiency, reduces the formation of certain pollutants, and decreases the amount of fuel required to reach the target process temperature. This option will be described in more detail in Chapter ??, but it is not analyzed in the study. The same chapter will also introduce a techno-economic analysis of a scenario in which hydrogen partially replaces fossil fuels, in line with the outlook of international organizations such as the IEA, which foresees a 9% share of hydrogen by 2050 [42]. This represents an interesting case for bringing the cement sector, particularly the Irish one, closer to future regulations that will require hydrogen integration and stricter CO₂ reduction targets.

These two scenarios will not be further investigated, as the focus of this thesis is the design of a renewable hydrogen production plant capable of supporting a significant scale-up of the hydrogen market in Ireland. Unlike options such as the UTIS patent or the 9% hydrogen substitution in the production process, which would only require minimal hydrogen volumes and would not justify the development of a dedicated production facility, this work considers a case study where substantial hydrogen quantities are required, thus motivating the design of a full-scale plant.

3.3 Carbon capture and utilization: production of sustainable methanol

Among the strategies aimed at decarbonizing the cement sector, the deployment of carbon capture technologies and the reduction of clinker content in cement are expected to achieve the largest overall CO₂ emission cuts by 2050, estimated at around 48% and 37%, respectively [33]. Carbon capture technologies are highly effective at reducing emissions from both the cement production process and fuel combustion, and their importance is growing as carbon pricing is expected to increase. Moreover, CCU provides a solution that transforms CO₂ from flue gases into useful products, offering a promising route for investments. By converting CO₂ into commercially valuable chemicals, high-emission industries can advance decarbonization efforts while contributing to a circular economy. This work concentrates on the production of methanol, a potential precursor of e-SAF, through the utilization of hydrogen and CO₂ captured from the plant. Assuming either an amine-based carbon capture system or a calcium looping process, a CO₂ capture efficiency was defined and used to determine the net amount of CO₂ available. Based on the stoichiometric reaction for methanol synthesis, both the hydrogen consumption and the methanol production were then calculated.

Methanol synthesis reaction

$$CO_2 + 3 H_2 \longrightarrow CH_3OH + H_2O$$

Assumption

 CO_2 capture efficiency 0.90 [32]

Table 3.3: CCU design assumption

In the cement sector, the potential use of captured CO_2 is often presented as an opportunity both to cut emissions and to reduce the overall cost of CCUS. However, most utilization pathways remain at an early stage of technological maturity and are far from large-scale commercialization [32]. As the estimation shows, and according to current studies, only a small fraction, typically less than 10%, of the CO_2 captured at a cement facility could realistically be transformed into marketable products [32]. The electrolyzer size and investment, in fact, is prohibitive in the development of this technological solution for CO_2 reduction.

Hydrogon	domand	actimation	for methano	leventhoeig
HVULUSEH	uemanu	esumation	ioi methano	1 9 / 11/11/2019

Molecular weight CO_2	44	g/mol
Molecular weight H_2	2	g/mol
Moles of CO_2	$1.28\cdot10^{10}$	mol
Moles of H_2	$3.85 \cdot 10^{10}$	mol
H_2 consumption	$7.69\cdot 10^4$	tons
$\mathrm{CH_{3}OH}$ production	$4.10\cdot 10^5$	tons
Electrolyzer estimated size	518	MW

Table 3.4: Hydrogen demand estimation for methanol synthesis

This graph, through 2024 electrolyzer cost data [43] and 2030 cost projection [44] shows the investment required for electrolyzer implementation versus the percentage of CO₂ reduction, for the case study cement plant. Reference CO₂ data were taken from the cement facility ETS allowances [45]. The 2030 trend of electrolyzer cost by CO₂ reduction share shows the potential of this technological application. Through substantial economy of scale for the electrolyzer, CCU may become more feasible.

According to the technology roadmap for cement industry, carbon capture solutions are expected to be integrated into cement production at commercial scale by 2030.[13]

For the above-mentioned reasons, this scenario was deemed not feasible and was not pursued further.

3.4 Transport fleet

The limited availability of fossil fuels will inevitably drive significant transformations in both the industry and transportation sectors. From a broader viewpoint, it is essential to drastically cut out fossil fuel consumption, while ensuring energy provision through renewable, efficient, and environmentally friendly systems.

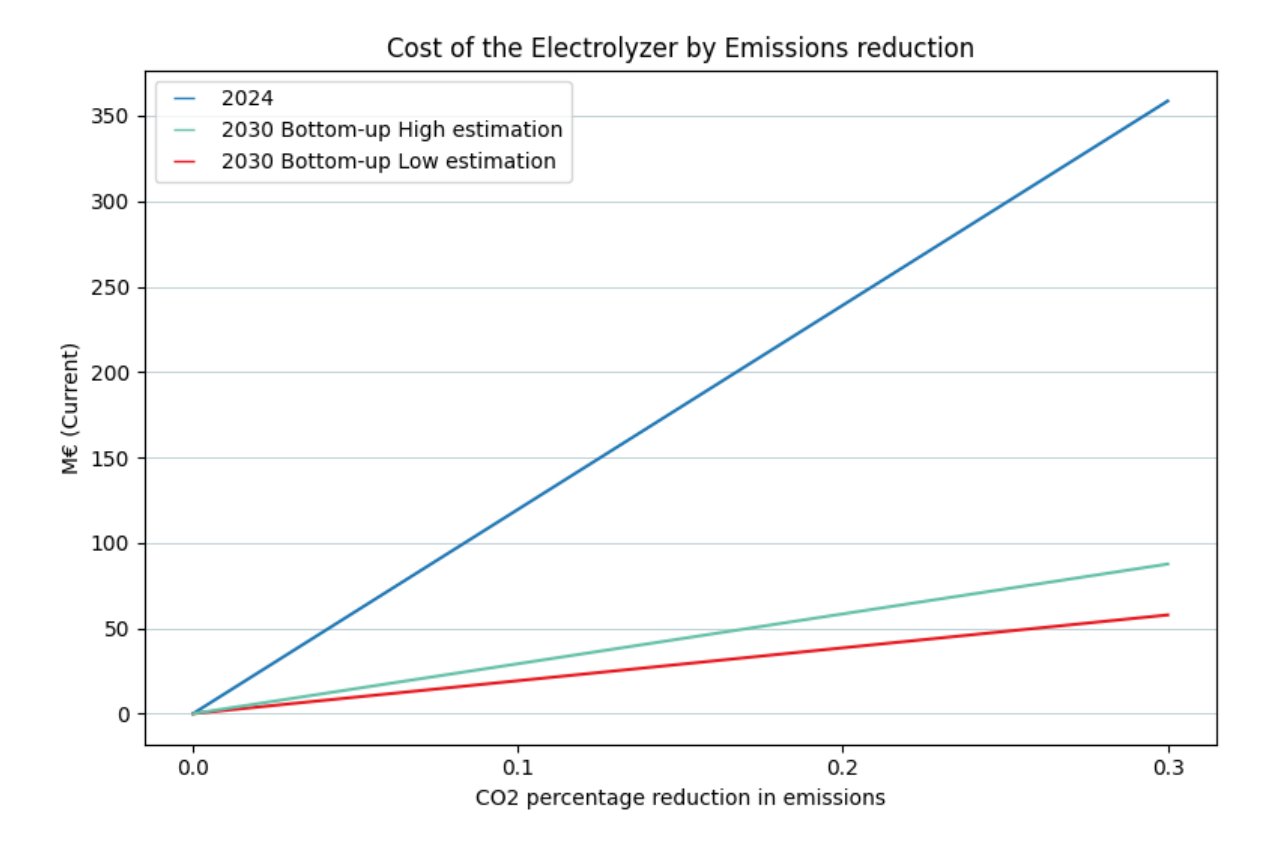


Figure 3.2: Cost projection of electrolyzer by emission reduction [43] [44]

Road transport, responsible for roughly 8 $GtCO_{2eq}$ globally [46] of 36,8 $GtCO_{2eq}$ emitted the same year [47], accounting for about 22% of all global CO_2 emissions, is among the most promising sectors for hydrogen and fuel cell applications. Using hydrogen as a fuel in fuel cell vehicles enables sustainable transportation without significantly altering current driving habits. However, realizing this potential depends on the systematic development of hydrogen infrastructure, which remains a considerable challenge.

Cement production facilities rely on a substantial fleet for delivering the final product and for internal operations within the quarry. Decarbonizing this fleet is a key step toward reducing the overall carbon footprint of the sector.

This scenario serves as the main focus of the present study. The aim is to develop a hydrogen production plant to supply a refueling station, with system size and components sized to meet the operational demands of the cement plant under investigation.

In the case under study, the fleet consists of trucks capable of covering national and regional distances, along with off-road trucks used on-site, which are typical vehicles for material transport in rough terrain.

To design the hydrogen refueling station, it is first necessary to analyze the fuel consumption of the transport fleet under consideration. Based on diesel consumption data provided by the company, the total annual mileage of the fleet was estimated, which was then used to calculate the corresponding annual hydrogen demand and to size a preliminary electrolyzer.

The following assumptions were adopted:

Assumptions for fleet H₂ demand

Diesel consumption heavy-duty trucks	33.1	$L/100~\mathrm{km}$	[48]
Hydrogen consumption FCET	9	kg/100 km	[49]
Electrolyzer efficiency	60	%	[41]
Electrolyzer operating hours	8260	h	

Table 3.5: Assumptions for fleet H₂ demand

Assuming to serve all of the fleet vehicles, the consumption amounts to 844.2 tons H_2 , corresponding to an electrolyzer size of about 6 MW. This preliminary estimation is essential because, as will be explained later, the Excel-based plant model uses the nominal power of the renewable generation system (PV + wind) and the electrolyzer as input variables, which can be adjusted according to the H_2 demand.

Hydrogen demand for transport fleet

Estimated hydrogen demand	844.2	tons
Electrolyzer estimated size	6	MW

Table 3.6: Hydrogen demand estimation for transport fleet

4 H₂ production plant model

An hourly model was implemented in Excel to simulate the behavior of the plant and to carry out the feasibility study. The hourly resolution was chosen to enable an hourly emissions balance, in line with regulatory requirements for installations commissioned after 2028, assuming that the construction of this plant will take place beyond that date.

The model enables the analysis of the storage system, quantifying its losses, and compares the hydrogen production with the demand from the served vehicles. From this, the amount of unmet hydrogen demand is determined, as well as the potential contribution of the electrical grid.

The model consists of the following main units:

- Renewable farm: photovoltaic and wind farm supply the electricity required for water electrolysis, with any surplus being fed into the grid.
- Battery: it stores surplus electricity and feed it to the electrolyzer when required.
- Alkaline electrolyzer: for hydrogen production through water electrolysis. Its production characteristics were analyzed as a function of the load factor.
- Hydrogen buffer tank: used as an intermediate storage after the electrolyzer.
- Compressor: powered by the grid, it compresses the hydrogen from the buffer pressure state to the low pressure storage, medium pressure storage or high pressure storage.

• Storages: two storages, for medium pressure levels (from 351 to 501 bar) and high pressure levels (up to 951 bar).

4.1 Power Farm

Solar energy generation is evaluated using power data from PVGIS sampled at the geographical location of the case study for a selected reference year, extracting the hourly energy output per unit. During the assessment phase, the per-unit energy is scaled according to the size of the plant, using the nominal power rating as the scaling factor.

Wind power generation, on the other hand, is based on data from www.renewables.ninja for the specific location considered. A sample Vestas V90 2 MW turbine was selected, and the electricity generation data were downloaded and normalized by dividing by the turbine's nominal power. These unit-generation values were then multiplied by the nominal power of the wind farm, which is a variable in the study and was selected, in combination with PV nominal capacity, to provide enough electricity to the electrolyzer to produce the designed amount of hydrogen.

4.2 Battery

The addition of a battery to the model provides more flexibility to the plant, especially because without it, a high curtailment of wind energy was necessary, due to hourly mismatch between turbines production and electrolyzer utilization.

The battery was implemented through several evaluations. Firstly, it was defined the battery nominal capacity in kWh and the battery charge and discharge nominal power in kW, together with the minimal level below which the battery can't be discharged (20%), to avoid deep cycling and, finally, the battery starting level of state of charge (20%).

After this, the potential surplus of energy was calculated as the difference between the total wind and solar generated electricity and the electrolyzer consumption. The resulting

Battery input parameters

Nominal capacity	kWh
Charge nominal power	kW
Discharge nominal power	kW
Minimum energy threshold	kWh
Initial state of charge	kWh

Table 4.1: Battery input parameters

value was checked with the maximum charge power, to compute the right value with respect to the limitations imposed.

To proceed with the evaluation of the hourly battery charge, the potential surplus was added to the starting state of charge of the battery, checking with the value of maximum capacity of the battery. If the calculated value exceeds it, the battery charges an energy that is the difference between the maximum one and the initial one.

To evaluate the battery discharge, firstly we set a treshold that defines when the discharge happens. This treshold is set at a value of 50% of utilization factor of the electrolyzer. This means that whenever the electrolyzer UF falls below this value, the discharge is triggered. The UF is a parameter that represents how much the electrolyzer is being use with respect to its maximum.

$$UF_{ely} = \frac{P_{consumption}}{P_{nominal}}$$

if
$$UF_{ely} < 50\% \rightarrow discharge\ battery$$

 $P_{consumption}$: Electrolyzer power consumption

 $P_{nominal}$: Electrolyzer nominal power

In this case, the UF of the electrolyzer is fixed at 50%. This value was compared with UF=20%, which represents the minimum load for electrolyzer activation, but, from an analysis of the battery, 50% was chosen because it ensures less electricity curtailment and more electrolyzer efficiency.

The discharge condition is triggered whenever renewable electricity production falls below the demand required to operate the electrolyzer at 50% UF. Once this condition is met, the difference between the renewable generation and the target demand is calculated. This missing energy represents the amount to be supplied by the battery.

The model then subtracts this energy request from the previous hour's state of charge. The new state of charge is compared with the battery's minimum energy threshold, set at 20% of total capacity. If the battery can discharge without dropping below this limit, the algorithm also verifies if the required discharge doesn't exceed the nominal discharge power. If both conditions are satisfied, the battery provides the missing energy to maintain the electrolyzer at the selected UF. Otherwise, no discharge is carried out.

The battery charge value is calculated as the difference between charging and discharging energy. A control is then performed to ensure that the resulting charge does not exceed the maximum storage capacity of the battery.

To provide a more intuitive indicator of the battery condition, the charge value is normalized by dividing it by the total capacity. This produces a dimensionless parameter ranging from 0 to 1, which directly represents the state of charge (SOC) of the battery.

Another parameter that was modeled is the curtailment of electricity, computed as the difference between the potential surplus and the battery charge. Finally, the missing represents the energy demand not met by the battery, keeping the UF at a value lower than 50%.

Two important aspects in the battery design are the discretization of the model, which prevents simultaneous charging and discharging, and the condition that if the battery cannot reach 50% UF, no discharge is performed, even though the battery could still

Battery model	
Potential surplus	kWh
Battery charge	kWh
Battery discharge	kWh
Battery charge value	kWh
State of charge	%
Curtailment	kWh
Missing	kWh

Table 4.2: Battery model

provide some energy to the electrolyzer.

4.3 Electrolyzer

The electrolyzer model is based on efficiency data provided by the manufacturer, which includes three efficiency curves as a function of the electrolyzer's production rate.

Four curves were constructed, starting from the ones provided, to describe the behavior of the electrolyzer. In particular:

- 1. Stack consumption as a function of overall consumption: isolates the stack energy consumption, to evaluate a parameter useful for evaluating the performance of the electrolyzer, which is the utilization factor.
- 2. Stack production as a function of overall consumption: through the stack efficiency it evaluates, from the overall input energy, the production in energy terms.
- 3. Stack consumption as a function of stack production: to integrate the use of electricity from the grid, we evaluate the maximum production allowed from flow rate constraints and, through this function, it's possible to evaluate the quantity of

electricity that the grid can provide.

4. Overall consumption as a function of stack consumption: to evaluate the total electricity from the grid, we have to go from the stack consumption back to the overall consumption.

By sampling the efficiency curves provided in arbitrarily points (20%, 25%, 50% and 100%), which represent the production rate, we obtain efficiency values for different configurations (stack efficiency, overall efficiency, balance of plant efficiency). The production energy of the stack and the overall consumption one can be computed through the production rate and relative efficiency values, while the stack consumption varies linearly with the production rate. A linear regression was applied to the set of pairs (overall consumption; stack consumption), obtaining the curve describing the consumption energy of the electrolyzer stack as a function of the overall consumption energy used.

The parameters obtained through the first function were then used for all the other three, in different combination.

In the plant model, when the electrolyzer is supplied with a total consumption value equal to the renewable energy generation, its theoretical hydrogen output can be estimated.

Finally, the total estimated renewable hydrogen production can be compared with the annual hydrogen demand, allowing for the adjustment of the electrolyzer's nominal power.

4.4 Buffer, compressors and storages

Once produced, hydrogen is first collected in a buffer tank at 31 bar (assumed as the electrolyzer outlet pressure), before being compressed and directed to the different storage units through a compressor.

Each storage tank can be filled up to its reference pressure and discharged down to a defined minimum pressure threshold.

Before reaching the storage units, the produced hydrogen is limited by:

Storage element	minimum pressure	maximum pressure
Buffer	7.9 bar	31 bar
Medium pressure storage	351 bar	501 bar
High pressure storage	351 bar	951 bar

Table 4.3: Buffer and storages parameters

- 1. Flow rate limitation, due to the maximum flow capacity of the system.
- 2. Maximum storage volume
- 3. Maximum discharge, due to the minimum pressure to be kept in the tank.

Two storage cascade configurations are possible:

- 1. Single storage configuration. In this setup, only one HP storage unit is used, due to the large amount of hydrogen that needs to be stored. The HP storage is directly connected to the buffer and is refilled whenever possible. Vehicle demand is supplied exclusively from the HP storage, by pressure equalization. The modelling of this configuration is, therefore, linear: the buffer provides hydrogen to the HP storage whenever possible, subject to flow, storage capacity, and minimum pressure constraints, while the HP tank directly meets the hourly vehicle demand. In this configuration, the HP storage acts both as the main supply to the fleet and as the reservoir for surplus hydrogen.
- 2. Two storage configuration. In this setup, a medium-pressure storage at 501 bar serves as the primary supply for the vehicle fleet, while the HP storage is used as auxiliary storage: it is filled during periods of surplus production and discharged only when the MP storage cannot fully meet vehicle demand. Each hour, the demand is first supplied by the MP storage, depending on availability. If the MP is not sufficient, the deficit request is transferred to the HP storage. If the HP can provide it, the system continues operating without interruption; otherwise, the

shortage is recorded as unmet demand. Similarly, if MP storage is full, the excess production is redirected to HP storage, which requires additional compression. In this way, the HP unit absorbs production peaks. In this case, the output from the buffer is determined not only by the demand of the MP storage but also by the demand of the HP storage, whenever the MP storage is already saturated. These operating rules ensure that: MP is always the primary source for refueling. HP intervenes only in two cases: to absorb excess production when MP is full; to cover shortages when MP cannot meet demand.

In both configurations, the buffer operates with a continuous discharge toward the main storage.

The compressor model compresses hydrogen from the buffer outlet pressure of 31 bar to the required pressure level in the two cases (501 bar for MP and 901 bar for HP). For simplicity, the compressor is supposed to be charged by grid energy.

The specific power of the compressor is calculated as the isentropic power of multistage compression divided by the maximum mass flow rate from the buffer. The total compression power is then obtained by multiplying the specific power by the actual mass flow rate.

$$P = \frac{RTZ}{MW\eta} \cdot \frac{\gamma N}{\gamma - 1} \cdot \left[\left(\frac{p_{out}}{p_{in}} \right)^{\frac{\gamma - 1}{\gamma N}} - 1 \right]$$

The compressor's annual electricity consumption was calculated as the sum of the hourly consumptions over the year. For each hour, the energy demand was obtained by multiplying the hydrogen flow from the buffer to the HP storage by the specific power of the compressor:

$$E_{consumption} = Q \cdot P$$

 $E_{consumption}$: hourly compressor's energy consumption [kWh]

Compressor's parameters

Z (hydrogen compressibility)	1	-
T (inlet temperature)	298	K
R (ideal gas constant)	8.314	J/k/mol
Molecular Weight H_2	2	-
\$eta (Compressor efficiency)	75	%
γ (diatomic constant factor)	1.4	-
N (number of compressor stages)	2	-
p IN	31	bar
p OUT	901	bar

Table 4.4: Compressor's parameters

Q: hydrogen flow rate to the compressor [kg/s]

$$P$$
: compressor's specific power $\left[\frac{KW}{kg/s}\right]$

The compressor model in the two-storage configuration follows the same structure, with only the inlet and outlet pressures and the flow rate varying. In this setup, two compressors are required: one to transfer hydrogen from the buffer to the MP storage, and another to further compress it from the MP to the HP storage.

4.5 Grid connection

Due to production variability and curtailment, the plant may at times experience a shortage of hydrogen relative to demand. The model therefore allows for the use of the electrical grid when both these situations happen:

1. The main storage level (expressed as a percentage of mass) falls below a defined threshold.

2. The buffer is unable to supply a flow to the storage.

In such cases, the grid intervenes providing a customizable level of electricity, which is regulated through a percentage addition to the utilization factor. The user can decide the said percentage, which will be added to the UF of the electrolyzer, allowing for more H_2 production. This limitation was introduced to design the grid intervention in order to comply with the reduction of CO_2 emissions given by the normative.

With this mechanism both the frequency and the amount of grid intervention can be regulated.

Apart from this limitation, the model can compute the theoretical maximum grid intervention to eliminate the H_2 shortages, through an inverse procedure that, from the renewable H_2 production computes the energy consumed and it confronts it with the maximum energy that the electrolyzer can consume.

4.6 Model corrections

During the model's implementation, two correction parameters were introduced in order to minimize errors arising from numerical interpolation. One is referred to production and the other to consumption. These errors occur when the reverse process for calculating the maximum grid intervention is carried out.

In the first case, it was observed that the inversely calculated hydrogen production values differed slightly from those calculated directly from the renewable system. To compensate for this effect, a correction coefficient was introduced and calculated for each operating hour of the electrolyzer. This correction coefficient is calculated as the ratio between the first production estimation and the expected one, evaluated from the related utilization factor.

In the second case, the overall consumption, which is equal to the energy supplied by renewables, is compared with the overall consumption estimated from the stack consumption, and the ratio is applied to each operating hour.

4.7 Refuelling profile

After assessing the preliminary hydrogen demand, as described in Section 3.4, the refueling profile was evaluated.

The refueling profile is dependent on the demand of the considered case. To model it, diesel consumption data, utilization profile of the vehicle and types of vehicles used in the facility were given from the company

The fleet was assumed to operate for 335 days per year, with the remaining 30 days of downtime distributed between August and December/January.

Assuming an on-board tank capacity of 30 kg of hydrogen at a storage pressure of 350 bar, the maximum mileage of a truck with a full tank was estimated as the ratio between the available fuel in the tank and the hydrogen specific consumption (0.09 kg_{H2} /km as defined in Section 3.4). Using data on the annual mileage and fleet size, the average daily distance travelled by a single vehicle was then derived. By comparing this daily mileage with the maximum mileage achievable with a full tank, the refueling frequency was determined, corresponding to approximately one refuel every two days for a single vehicle (half the fleet in a day).

FCET characteristic

On board storage tank	30 kg	[36]
Operating pressure	350 bar	[36]
Specific consumption	$0.09~kgH_2/\mathrm{km}$	[41]
Average km travelled (tank size/specific consumption)	333 km	

Table 4.5: FCET characteristic

For the dispenser characteristics, 3.6 kg/min of available flow was assumed and the time

necessary for one refuel was computed as the flow from the dispenser divided by the 30 kg of volume of the on-board tank.

$$t = \frac{\dot{G}}{V} = 8.33 \; min/truck$$

t: time needed for one refuel

 \dot{G} : maximum discharge flow from the dispenser

V: volume of the FCET storage

$$t_{eff} = \frac{t}{\eta_{ref}} = 10 \ min/truck$$

 t_{eff} : effective time for one refuel

 η_{ref} : $\frac{t}{t_{available}}$: operating refueling efficiency

An operative efficiency of about 0.83 was considered, which represents the time needed for the switch between one truck and another that must be refueled. In the end, 10 min was the resulting time for one refuel. To calculate the number of dispensers needed, considering the time needed for one refuel and the number of vehicles to be refueled, it was determined that at least 2 dispensers are needed.

Dispenser characteristics and refuel frequency estimation

Flow	3.6 kg/min	[38]
Operating pressure	350 bar	
Operating efficiency	0.83	
Time of 1 refuel	10 min	
Number of dipenser	2	

Table 4.6: Dispenser characteristics and refuel frequency estimation

At this point, the hourly refueling profile in a typical day needs to be determined. It was

assumed that the preferred moment for refueling would be the evening, but, in order to not oversize excessively the refueling station, another moment during the morning was considered, since there is a large fleet to be served. The number of refuels in an hour is simply computed as the time needed for 1 refuel multiplied by the time available (e.g. 1 hour) and by 2, the available dispensers.

$$N = \frac{t_{av}}{t_{eff}} \cdot n = 12 \ refuels$$

$$G_{H_2} = V \cdot N = 360 \ kg_{H_2}/h$$

N: number of refuels in one hour

 t_{av} : time available in one hour (60 min)

n: number of dispensers available

 G_{H_2} : H_2 consumption in one hour of refuel

Reference day hourly H₂ consumption

	, <u>–</u>	
05:00:00	08:00:00	36 refuels
	3 h	$1080~kg_{H_2}$
		$360 \ kg_{H_2}/h$
16:00:00	20:00:00	48 refuels
	4 h	$1440 \ kg_{H_2}$
		$2520~kg_{H_2}/day$
тот		$360 \ kg_{H_2}/h$
H_2 annual consumption		$844.2\ tonnes_{H_2}/h$

Table 4.7: Reference day hourly H₂ consumption

This refueling profile can be customized and changed, modifying the hourly consumption fed to the model as well. This case represents a baseload scenario, with assumptions made arbitrarily. Other scenarios will be presented in the sensitivity analysis.

4.8 Reduction of CO₂eq emissions

The Delegated Regulation (EU) 2023/1185 sets the criteria for considering hydrogen produced from renewable sources as a RFNBO under Directive (EU) 2018/2001. It also defines the methodology for calculating GHG emission reductions associated with the use of such fuels.

The regulation requires that the reduction of GHG emissions from fuels produced from recycled carbon must be at least 70% compared to the reference fossil fuels. This minimum threshold applies to all types of recycled carbon fuels, including those used for renewable hydrogen production

GHG emission reductions are calculated over the entire life cycle of the fuel using the formula:

$$GHG\ reduction = \frac{E_f - E}{E_f}$$

Where:

 E_f : total emissions from the reference fossil fuel (94 g CO_{2eq}/MJ)

E: total emissions generated by renewable fuel

By calculating the 30% of the benchmark and then through the H_2 lower heating value, we obtain the maximum emissions allowed for kg_{H2} . In the model, the calculated maximum allowed emissions were multiplied by the hydrogen production for each specific hour and applied across all operating hours. This provides the maximum emissions permitted for that hour.

Emissions from grid electricity use were calculated by multiplying the Irish grid emission factor by the modelled hourly grid electricity consumption.

H₂ emissions

Benchmark	94	gCO_{2eq}/MJ	[50]
GHG reduction	70	%	[50]
Maximum emissions allowed	101.52	$kgCO_{2eq}/\mathrm{MWh}$	-
Maximum emissions allowed for kg_{H_2}	3.39	$kgCO_{2eq}/kg_{H2}$	-
Irish grid emission factor	0.44	tCO_{2eq}/MWh	[51]

Table 4.8: H_2 emissions

Through an hourly confront between these two values, it is possible to evaluate if the emissions produced by grid use are below the threshold or not, and therefore if the hydrogen produced can be considered renewable fuel.

4.9 Python implementation

As further advancement in the work, the plant production model was also converted on the python programming language, to facilitate future work and techno economic evaluations.

Four open-source libraries were used, related to the data analysis part:

- 1. Numpy: the model is based on calculations made on large vectors that represent quantities spread hourly in an entire year;
- 2. Pandas: to read and arrange data from files;
- 3. Sklearn.kit: for data regression and polynomial fit $(2^{nd} degree)$;
- 4. Matplotlib: various graphs related to data analysis

In addition, the Object-Oriented programming paradigm was used, to make the code more understandable, creating a simplified behavioral model of each component. In the H₂ production plant model

following paraphs, a detailed explanation of the implemented code and working principle

will be carried out.

4.9.1 Electrolyzer

Electrolyzer class is a full functional model of an electrolyzer, that gives different infor-

mation by giving different inputs. When the class is initialized, four imputs are needed

in order to provide a characterization of the electrolyzer, namely:

1. The nominal power of the electrolizer (kW)

2. The electrolizer efficiency curve (giving a production rate, related to nominal power,

it returns the electrolizer efficiency)

3. The electrolizer balance of plant efficiency curve (by production rate)

4. The electrolizer overall efficiency curve (by production rate)

During the initialization of the class, a production rate sample defined between the values

0.1 and 1 was created.

With this sample it was possible to obtain the corresponding values of the effective power:

$$P_{eff} = P_{nom} \cdot r$$

 P_{eff} : effective power

 P_{nom} : nominal power

r: production rate

The hydrogen production is obtained by:

$$H_{2,prod} = P_{eff} \cdot \eta$$

 $H_{2,prod}$: hydrogen production

 η : electrolyzer efficiency

The overall consumption is obtained as:

$$E_{cons} = \frac{H_{2,prod}}{\eta}$$

 E_{cons} : overall consumptio of electrolyzer

Requesting a 2^{nd} degree polynomial fit, the following functions were found:

- Effective power by overall consumption (Figure 4.1)
- Production by overall consumption (Figure 4.2)
- Effective power by production (Figure 4.3)
- Overall consumption by effective power (Figure 4.4)

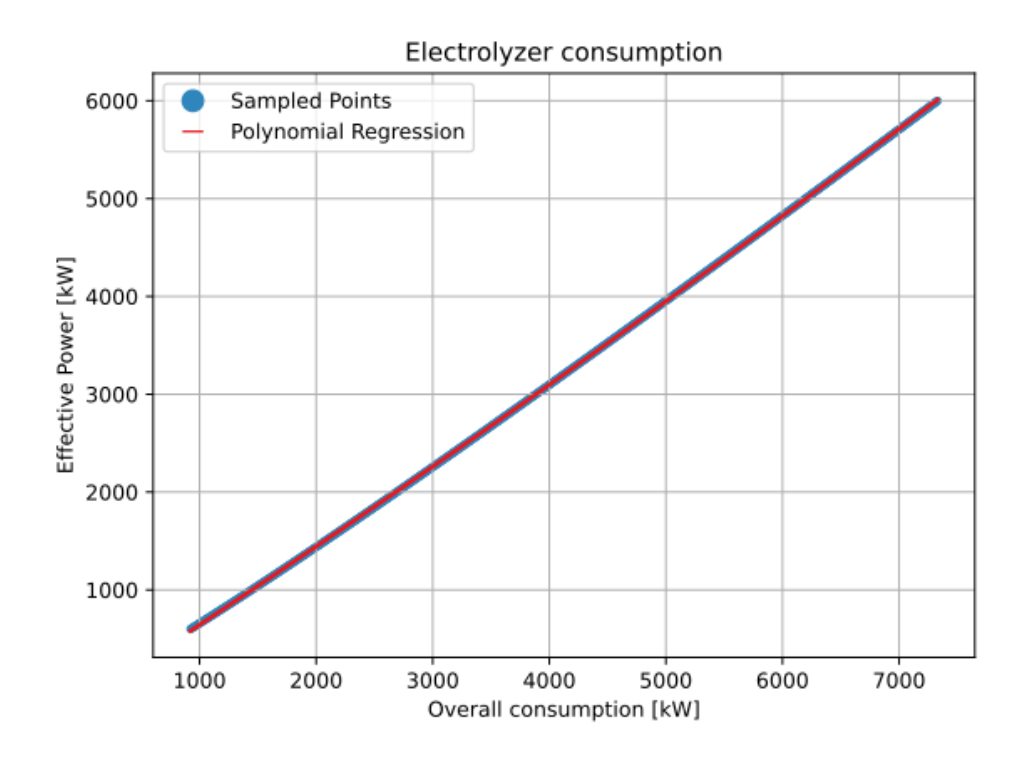


Figure 4.1: Effective power by overall consumption

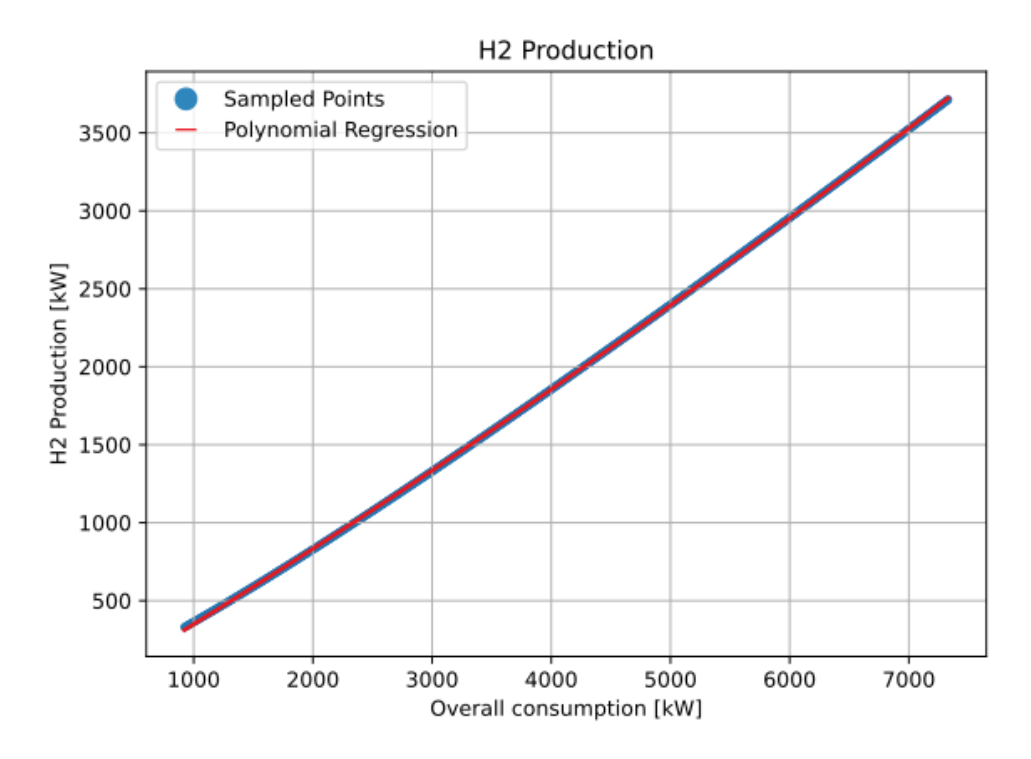


Figure 4.2: Production by overall consumption

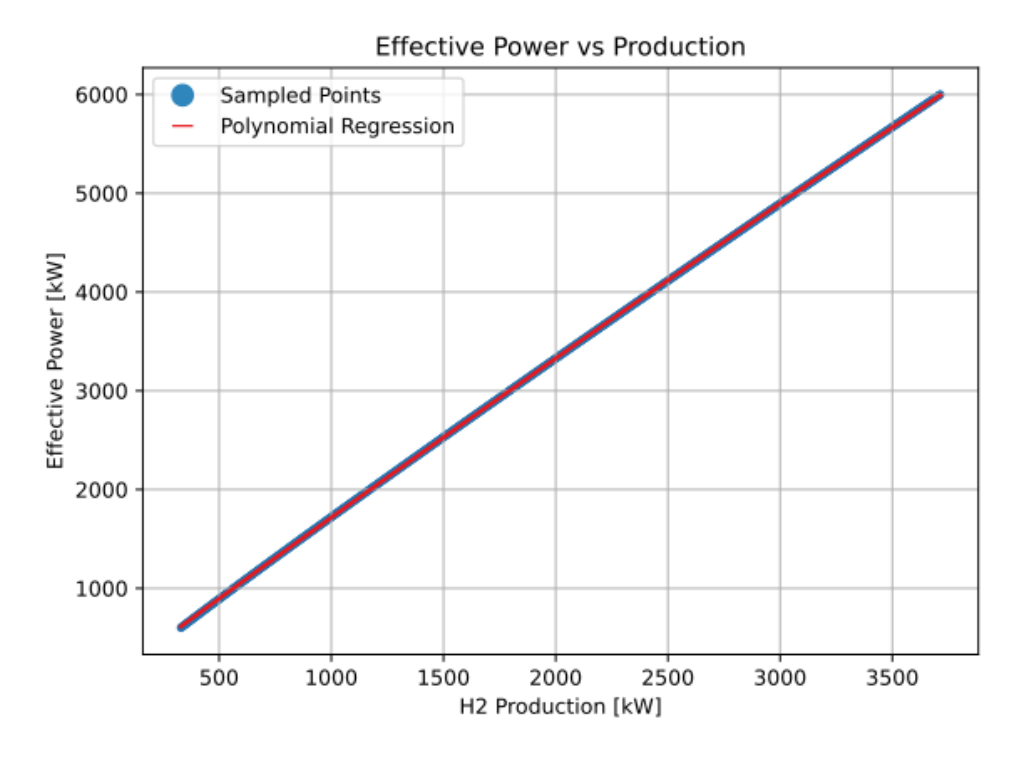


Figure 4.3: Effective power by production

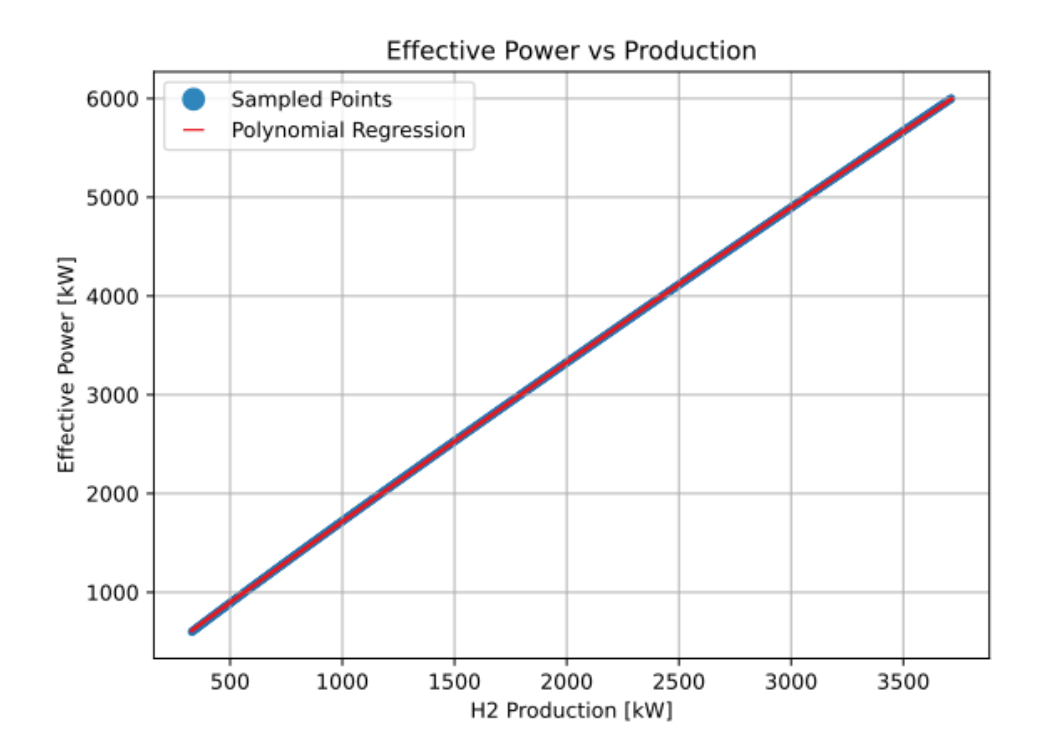


Figure 4.4: Overall consumption by effective power

All the evaluated regression models were stored in four class variables (members of the class) as lambda functions. This way, whenever needed, the *Electrolyzer* class can internally call these functions to predict the required value (or array) for the computation.

By designing, the *Electrolyzer* class, once initialized, shall be used by calling the methods that it exposes:

- Get Effective Power: giving the load will return the effective power [kW]
- Get Production: giving the load percentage will return the hydrogen production [tons]
- Get Ely BOP Consumption: giving the load percentage will return the consumption [kWh]
- Get Overall Consumption: giving the load percentage will return the overall consumption
- Get Effective Power by Consumption, found with the regression model during the initialization phase

- Get Production by Consumption, found with the regression model during the initialization phase
- Get Effective Power by Production, found with the regression model during the initialization phase
- Get Consumption by Effective Power, found with the regression model during the initialization phase

4.9.2 Renewable Farms

The energy provided by the renewables was modelized as unique class, called *Renewable Farms*.

During the initialization phase of the *Renewable Farms*, the user shall provide the nominal power of the photovoltaic farm and the wind farm.

The initializer locates the PVGIS and the Renewable Ninja files, containing the hourly power of a sample plant, and builds the model of the photovoltaic farm and the wind farm.

Each farm model can be queried, obtaining two information:

- 1. The power produced
- 2. The power produced per unit

4.9.3 Battery

To model the battery, a Battery class was implemented, by giving the following parameters as imputs:

- Nominal Power in charging phase
- Nominal Power in discharging phase

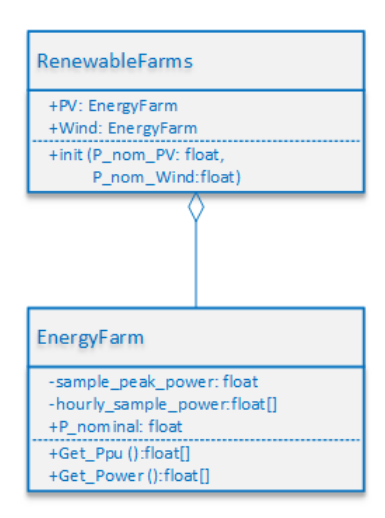


Figure 4.5: Renewable farms class diagram

- Charge efficiency
- Discharge efficiency
- Minimum charge level
- capacity
- Initial charge level

The battery shall be connected to a charge source, the battery input energy, and a discharge source, the battery requested energy.

The battery will try to provide an amount of energy as close as possible to the requested energy output.

The Battery class, once created, is meant to be used by calling two methods:

- 1. Get discharge power: giving an input energy, and an output request, the method will return the discharge power that the battery can provide to satisfy the request
- 2. Get state of charge: giving input energy and an output request, the method will return the state of charge due to the battery interaction with the system

4.9.4 Compressor

The *H2Compressor* class represents a physical compressor that operates between two fixed pressures (inlet and outlet).

To initialize the specific compressor the user shall provide the following parameters:

- The inlet temperature of the gas
- The compressor efficiency
- The compression stage number
- The inlet pressure
- The outlet pressure

In addition, the H2Compressor class stores constant parameters related to the hydrogen compression:

- The compressibility factor (Z)
- The ideal gas constant (R)
- H₂ molecular weight
- The diatomic constant factor (γ)

The class can evaluate its specific power, and, giving a target invariant mass flow rate, its energy consumption in one hour.

4.9.5 Storage

The storage model is composed of two classes, the H2GasProperties class, and the GasStorage class.

The first class has the responsibility to read 6 files in which hydrogen properties related to the temperatures of 0°, 5°, 10°, 15°, 20° and 25° are contained.

The class also will provide the function to extract an array of 6 entries, containing the hydrogen density at the six-sample temperature, by giving the reference pressure.

4.9.6 Plant model

The plant model builds the renewable energy plant, using the data, by giving some input parameters and it currently consists of a wind farm, a solar farm and an electrolyzer.

The goal is to estimate the hydrogen production of the farm.

By combining all the component it is possible to evaluate the annual production of the plant, by following steps:

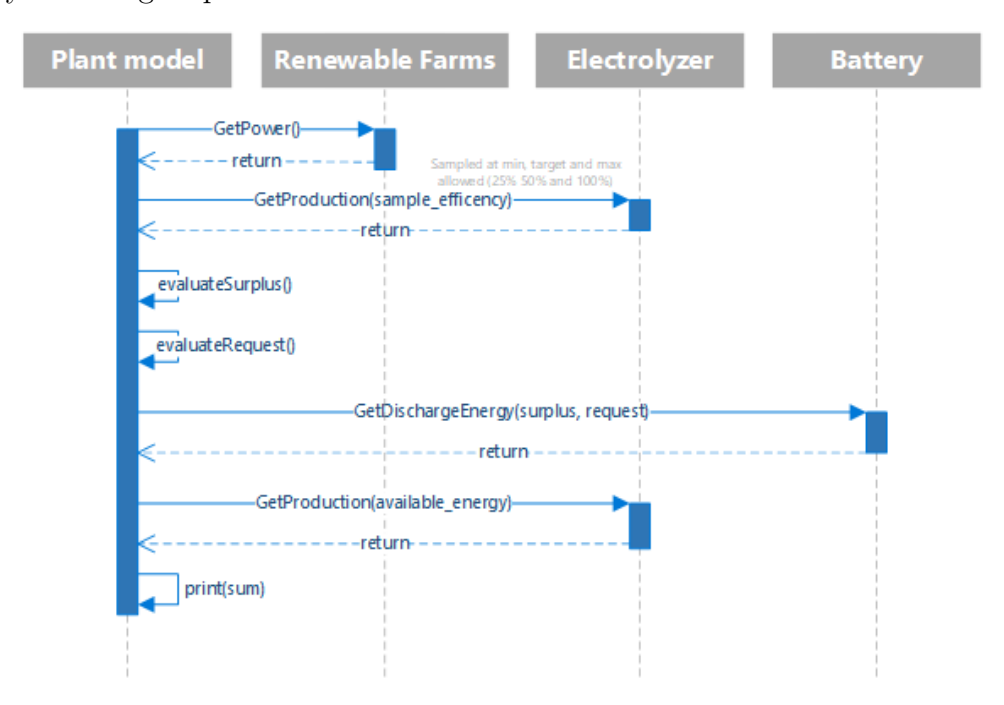


Figure 4.6: Plant model sequence diagram

- Evaluate the power provided by the renewables
- Obtaining the production values at 25%, 50% and 100% of the production rate
- Evaluating the renewables surplus (energy exciding the 100% of production rate) or energy below 25% (not suitable for use)

- Evaluating the request (energy needed to reach the 50% of production rate)
- Evaluating the available energy (renewable energy + battery discharge energy)
- Calculating the production by the available energy.

5 Plant base-case design and techno economic assessment

This chapter presents and discusses the results derived from the developed model. The analysis is conducted from two complementary perspectives: on one hand, the technological aspects, including system performance, size and operational behavior; on the other hand, the economic aspect, with a focus on investment costs, resources costs, and overall feasibility. The goal is to have a base-case design with fully renewable electricity supply, which will be optimized in the sensitivity analysis.

In this design, a small percentage of unmet demand is considered acceptable, in order to analyze how this parameter depends on system design choices and associated costs. A further development of the model will instead be presented and assessed under the condition that hydrogen production fully matches consumption.

5.1 Cost analysis

A detailed cost assessment of the plant components is essential to evaluate key performance indicators such as the Levelized Cost of Hydrogen and the Levelized cost of Energy of the investment. To this end, each component of the system was analyzed, referring to scientific literature data and findings, with the primary objective of identifying both capital expenditures and operating expenditures.

5.1.1 Renewable power farm

The cost analysis of the renewable farm was carried out using data from the IRENA Renewable Power Generation Cost in 2024 report. The total installed specific cost was taken as the European average for the reference year and subsequently converted from USD to EUR, applying the exchange rate of December 2024. By multiplying the specific installed cost by the plant size, the total CAPEX of the investment was obtained.

For PV OPEX costs, the European average value was chosen and then converted from USD to EUR.

For wind OPEX costs, the IRENA report does not provide European average values. Moreover, while Irish data were not available for the total installed costs, they were reported for wind OPEX. Therefore, the Irish value was used in this specific case. The OPEX was assumed under a full-service scheme (including both initial and renewal contracts). However, it should be noted that in recent years there has been a tendency to move from long-term full-service agreements to more flexible partial-service contracts, especially for aging fleets where maintenance costs are higher.

PV cost analysis-assumptions

Specific Total Installed Cost	779.00	USD/kW	[52]
USD value in EUR 2024	1.039	-	-
Specific Total Installed Cost-EUR	749.83	€/kW	-
Specific opex	7.30	USD/kW	[52]
Specific opex PV	7.03	€/kWp/y	-

Table 5.1: PV Cost analysis-assumptions

Wind cost analysis-assumptions

Specific Total Installed Cost	1659	USD/kW	[52]
USD value in EUR 2024	1.039	-	-
Specific Total Installed Cost-EUR	1596.88	€/kW	-
Specific opex	21	USD/kW	[52]
Specific opex PV	20.21	€/kWp/y	_

Table 5.2: Wind cost analysis assumptions

5.1.2 Battery

For the battery cost assessment, reference was made to the techno-economic analysis conducted by Kebede et al. [53] comparing lithium-ion and lead-acid batteries for stationary energy storage applications. Lithium-ion technology was chosen for this study, as it currently leads the market thanks to its superior energy density, efficiency, scalability, and longer operational lifetime.

The charging energy was obtained from the model results, and the number of cycles per year was computed as the ratio between the annual charging energy (in MWh) and the net usable energy per cycle. For simplification, it was assumed that each charging cycle is complete, spanning from the minimum to the maximum state of charge:

$$N = \frac{E_{charge}}{E_{max} - E_{min}}$$

N: number of charge/discharge cycles per year

 E_{charge} : charging energy (model's result)

 E_{max} : maximum charging energy

 E_{min} : minimum discharging energy

By comparing the calculated annual cycles with the number of cycles corresponding to the

maximum DoD, which represents the end-of-life of the battery, beyond which its capacity and performance are significantly degraded, the battery lifetime can be estimated. The results show a battery lifetime of 20 years and, considering that it represents also the investment's lifetime, no battery replacement was considered.

As suggested in the reference paper, no operation and maintenance costs were considered.

Battery cost analysis-assumptions

Specific Cost	463.22	USD/kWh	[53]
Replacement Cost	413.00	€/kWh	[53]
Installation and Indirect Costs	16.84	€/kW	[53]
Cycles number at max DoD	3000	-	[53]

Table 5.3: Battery cost analysis assumptions

5.1.3 Electrolyzer

The electrolyzer CAPEX was derived from a comparison between the state of the art in specific electrolyzers costs and Marocco et al [54] study was chosen as reference value. The cost was computed as the specific cost multiplied by the electrolyzer size.

OPEX was assumed to be fixed at 4% of CAPEX, while stack replacement costs were set at 26.7% of the initial CAPEX. A stack lifetime of 60 000 operating hours was considered, and the replacement frequency was calculated by comparing this lifetime with the total annual operating hours.

5.1.4 Compressor

To compute the compressor cost, two references were considered, from a cost quotation made available by the research team. A linear interpolation was carried out to obtain the compressor's cost for the case under study.

Electrolyzer cost analysis-assumptions

Specific Cost	2000	USD/kWh	[54] [55]
Stack replacement Cost	26.7	%	[54]
Fixed opex (% of inv. Cost)	4	%	[54]
Variable opex (% of inv. Cost)	4	%	[54]
Operating hours	76932	-	[54]

Table 5.4: Electrolyzer cost analysis assumptions

Available costs quotation-compressor				
Compression power	5.5 kW	235.300	€	
Compression power	11 kW	240.600	€	

Table 5.5: Available costs quotation for compressor

The annual electricity cost was then determined by multiplying the yearly total consumption, model's result, by the grid electricity price.

OPEX were assumed to be fixed, corresponding to 3.5% of the capital expenditure CAPEX.

Finally, the total CAPEX was obtained by adding installation and indirect costs to the base equipment cost.

Compressor cost analysis assumptions

Specific cost	1179	€/kW
Installation cost	28	%
Indirect cost	36	%

Table 5.6: Compressor cost analysis assumptions

5.1.5 Storage

The cost analysis of the buffer and storages was carried out using reference specific costs associated with the corresponding pressure level. The storage cost was obtained by multiplying the storage capacity by the specific cost at the given pressure. The final CAPEX also included installation and indirect costs.

Storage reference specific cost |250 bar| $500 \in /kg_{H2}$ 300-1000 bar $1000 \in /kg_{H2}$

Table 5.7: Storage reference specific cost

In the refueling station, the dispenser cost was included, representing two H_2 dispensers.

Hydrogen Refueling Station				
Dispenser	472 000	€	[57]	
Dispenser lifetime	10	years	[57]	

Table 5.8: Hydrogen Refueling Station

5.2 Levelized cost of energy/hydrogen

The Levelized Cost of Hydrogen approach derives from the well-established Levelized Cost of Energy methodology, extensively applied in the renewable energy field. In this framework, the total life cycle cost of a technology is normalized by its lifetime energy output, giving a unit cost of energy. According to IRENA, the LCOE can be expressed as shown in Equation

$$LCOE = \frac{\sum_{t=1}^{n} \frac{I_t + M_t + F_t}{(1+r)^t}}{\sum_{t=1}^{n} \frac{E_t}{(1+r)^t}} [58]$$

 I_t : initial investment cost for year t

 M_t : maintenance cost in year t

 F_t : fuel cost in year t (considered zero for renewables such as wind and solar)

 E_t : energy generation in year t

r: discount rate

n: lifetime of the system

The LCOE method offers a valuable reference for comparing various energy technologies and is not limited to renewable sources. It has also been widely used to assess the cost of hydrogen production. Because hydrogen output can be quantified in energy terms, its cost can be expressed either per unit of energy or per kilogram, following a similar approach to that used for electricity.

In this analysis, electricity generation and hydrogen production were evaluated considering different WACC for each of them, since the investments carry different risks. The LCOE of wind and PV energy was determined as the electricity price that results in a NPV equal to zero over the project lifetime, ensuring recovery of the initial capital investment. The LCOE takes into account the share of grid energy used and, with reference to its cost, it adds its contribution to the renewable one.

The discount rate, derived from the Weighted Average Cost of Capital, was set at 3.3% [59], reflecting the expected financial return and the project-specific risk. A project lifetime of 20 years was assumed.

Other investment parameters

Weighted average cost of capital	3.3	%	[59]
Project lifetime	20	years	-
Cost of electricity from grid	230	€/MWh	[60]

Table 5.9: Other investment parameters

To estimate the cost of electricity from PV and wind, an average LCOE was computed based on the productivity and surplus generation from each technology and then multiplied by the corresponding amount of energy supplied by both farms to the electrolyzer. In case of only wind or only PV generation, the same procedure was applied, resulting in only one LCOE rather than an average between two.

To evaluate the Levelized Cost of Hydrogen, defined as the ratio between discounted cash flows and discounted hydrogen output, all main components of the infrastructure were considered (wind farm, electrolyzer, buffer, storage unit, and HRS/dispensers). For each component, CAPEX, fixed OPEX and variable OPEX, related to electricity consumption from both the grid and renewable sources, were assessed.

OPEX were divided into three categories: annual fixed maintenance costs; variable electricity costs (with separate contributions from the grid and from PV/wind, weighted according to their respective shares); and the cost of demineralized water required for electrolysis.

The other parameters adopted for the calculation are:

Other parameters

Weighted average cost of capital 6% [61]

Table 5.10: Other parameters

In the cash flow analysis, the parameters described above were considered, while no revenues were included, because hydrogen is used internally.

5.3 Base-case plant design

The base-case design was developed to establish a reference configuration of the system, providing indicative component sizes and performance metrics. This configuration serves as a benchmark around which the sensitivity analysis can be carried out, allowing the

identification of the most influential design parameters on the system's techno-economic performance, particularly LCOH and unmet demand.

The design was carried out by individual variation of key system components:

- Renewable energy mix
- Battery size
- Storage volume

Subsequent observation of the impact of each variation on the target metrics allowed to select an operating size.

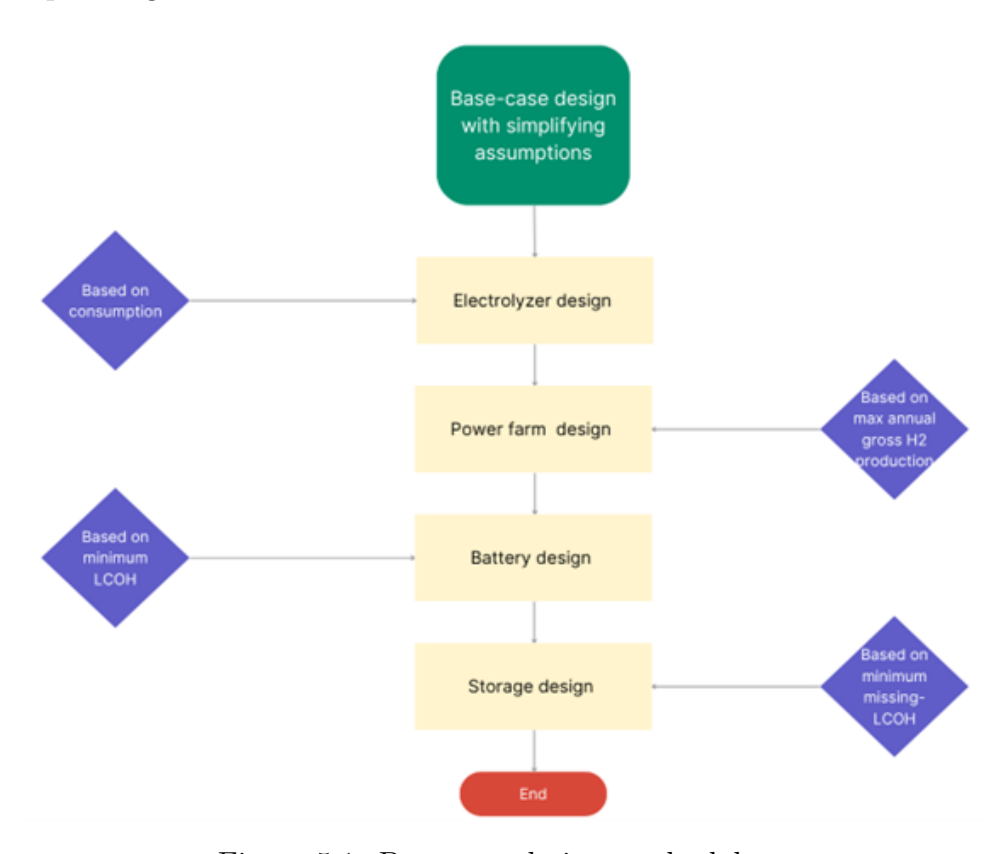


Figure 5.1: Base case design methodology

The starting point of the analysis was the electrolyzer size previously estimated. In theory, an alkaline electrolyzer with a nominal capacity of 6 MW would be sufficient to meet the projected hydrogen consumption. However, the electrolyzer implemented in the hourly model accounts for the overall system efficiency, which also includes the auxiliary

components required for operation. In this case, the efficiency is lower than the one assumed in the preliminary sizing, which referred only to the stack.

Furthermore, the efficiency of the electrolyzer, both at stack level and system level, depends on the operating load, expressed as the production rate relative to its maximum capacity. The system achieves its highest efficiency when running at full capacity, while partial load operation results in lower efficiencies. Consequently, on days with limited renewable electricity generation, the electrolyzer not only produces less hydrogen due to reduced input power but also operates less efficiently.

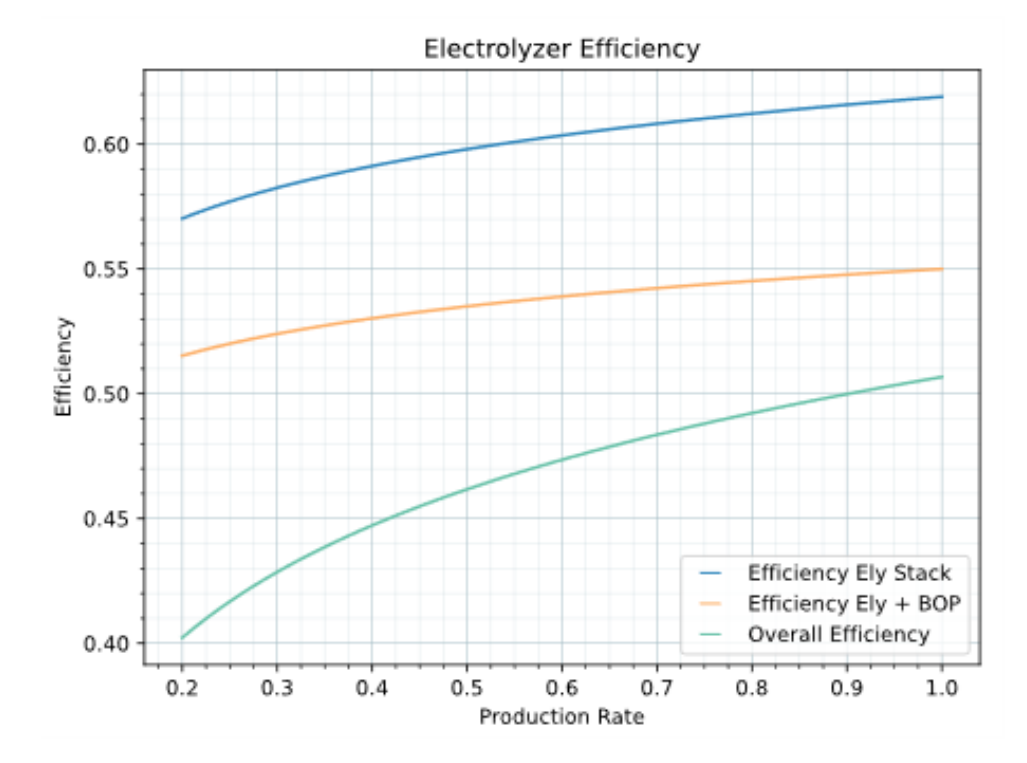


Figure 5.2: Electrolyzer efficiency with respect to production rate (load)

As a consequence, it is preferable not to oversize the electrolyzer, but rather to operate it at full load for the longest possible time. Under the assumption of continuous operation at full load, the maximum overall efficiency can be achieved, leading to an estimated required capacity of 7 MW.

The following step concerned the sizing of the power farm. In the model, multiple simulations were performed, keeping the electrolyzer size fixed, and considering no battery and storage contribution, and the results in terms of installed capacity and gross hydrogen

Elctrolyzer cost analysis results			
Size	7	MW	
Electrolyzer CAPEX	14	M€	
Opex (fixed+variable)	1.1	М€/у	
Substitution	3.7	М€	
Electrolyzer substitution frequency	9.5	years	

Table 5.11: Electrolyzer cost analysis results

production were collected and analyzed.

The following graph reports the hydrogen production as a function of the share of solar energy in the renewable mix, while keeping the total installed capacity constant.

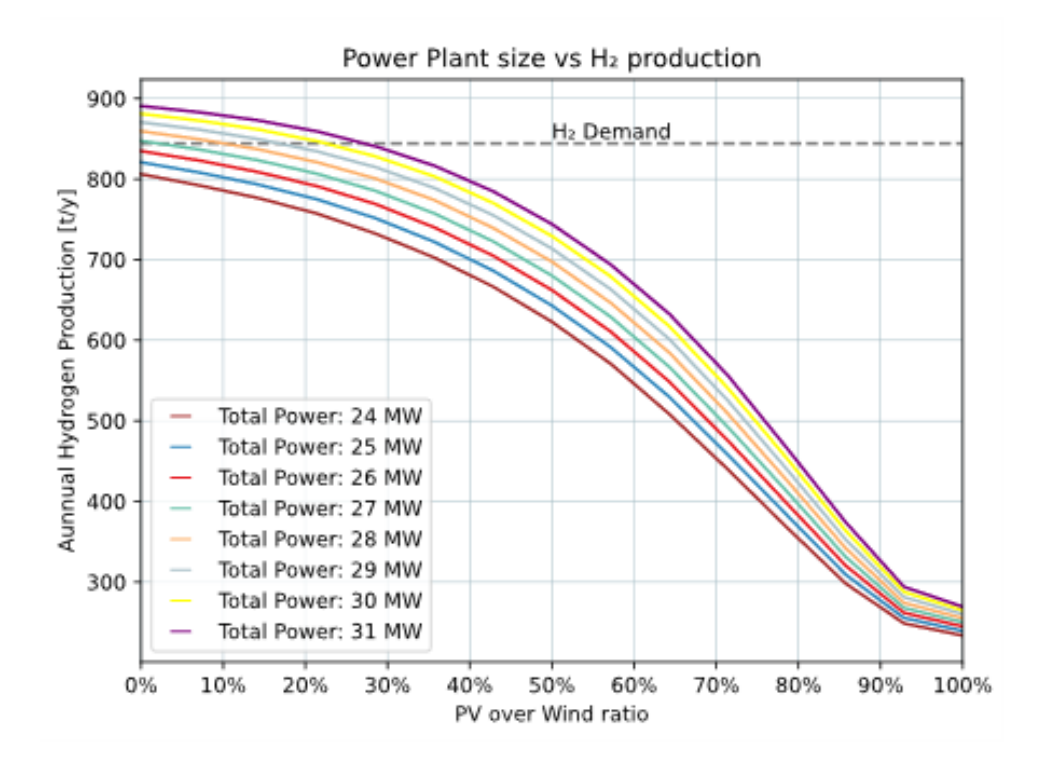


Figure 5.3: H₂ production with respect to solar share, fixed capacity

From this analysis, two main insights were obtained:

1. Reference nominal capacity. The capacity was selected as the one ensuring a production value which is the same of consumption. Among the two feasible values,

- 28 MW and 29 MW, the higher capacity was chosen, in order to compensate for potential flow losses within the plant.
- 2. Solar energy contribution. The results clearly show that increasing the share of solar energy, while keeping the same total capacity, leads to a decrease in overall hydrogen production.

Based on these outcomes, the base-case scenario was defined as a power farm composed exclusively of wind energy, as this configuration maximizes the renewable electricity available for hydrogen production.

Wind farm cost analysis results			
Size	29	MW	
Single turbine power	6	MW	
Number of turbines	5	-	
Wind farm Capex	46.31	M€	
Fixed Opex	0.59	М€/у	

Table 5.12: Wind farm cost analysis results

The battery design was assessed through several model simulations.

The figure 5.4 illustrates the battery sizing curve, where the capacity is varied between 0 and 30 MWh and the corresponding LCOH is evaluated. LCOH was selected because it carries not only informations regarding the economic aspect, but also about the net hydrogen produced. The curve 5.4 shows three distinct trends. Initially, when starting from the case without storage, the introduction of a small battery causes a sharp increase in costs, reaching nearly 10 €/kg at around 6-7 MWh of capacity. In this range, the battery's effect is purely detrimental due to a modeling constraint: it can discharge energy only if it is sufficient to raise the electrolyzer utilization factor to 50%; otherwise, it remains idle. Consequently, the battery is too small to meaningfully support hydrogen production, and the additional CAPEX is not offset by a significant reduction in hydrogen

missing events, making this configuration less competitive. After this peak, however, the curve shows a steep decrease: between 7 and 12 MWh, the battery provides relevant system benefits, especially in terms of hydrogen production, and the LCOH drops again to approximately $8.6 \in /kg$. This represents the optimal battery range, where the cost reduction balances the additional investment. Beyond 12 MWh, the curve increases gradually up to 30 MWh, indicating that further enlarging the battery leads to marginal benefits but increasing costs, and therefore to less convenient configurations.

Overall, the analysis highlights that the integration of a battery can improve the competitiveness of the system only if properly sized. In particular, the optimal configuration is obtained with a capacity of about 11 MWh, which minimizes the LCOH while reducing un-met demand percentage compared to the no-battery case.

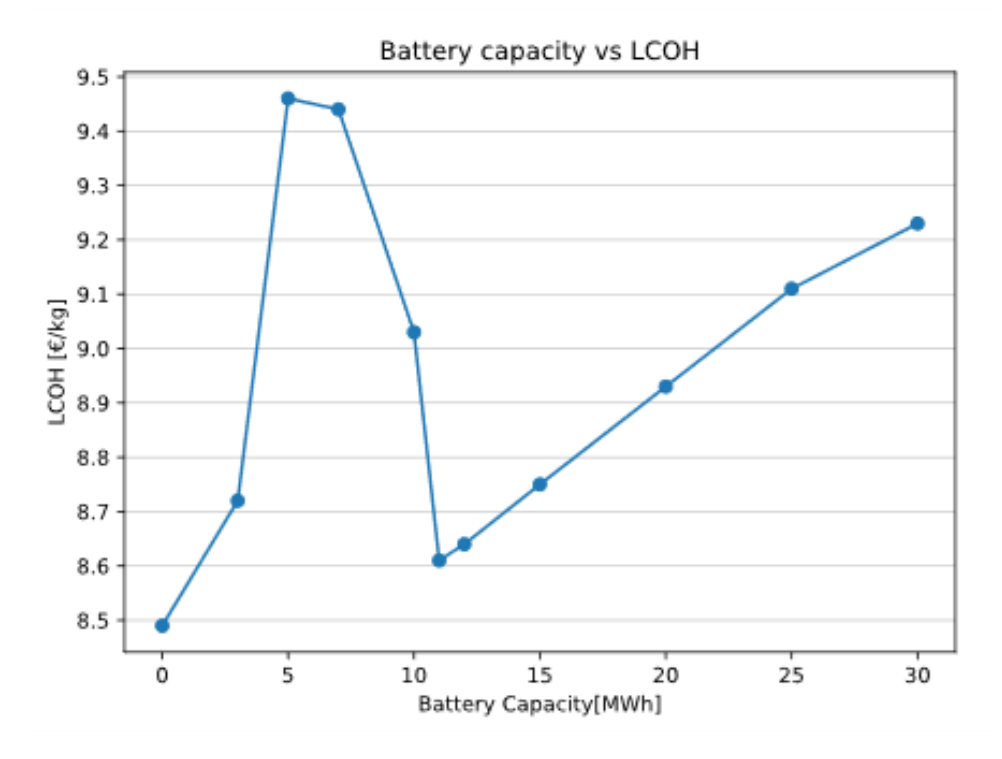


Figure 5.4: Battery size versus LCOH

The percentage of demand not met, due to the configuration of the system, is an important parameter considered. Being in fact intermittent the production of electricity, and therefore of hydrogen, it is inevitable the mismatch between production and consumption, which will not happen at the same time. In some cases, hydrogen production may exceed demand due to high wind availability, leading to curtailment when the storage

Battery cost analysis results

Nominal capacity	11	MWh
Charging energy	1.32	GWh
Number of charging cycles in a year	150	years
Battery life	20	М€
CAPEX	5.28	М€
Opex	0	М€

Table 5.13: Battery cost analysis results

units reach their maximum capacity. Conversely, during periods of low wind, production may be insufficient to meet demand, resulting in unmet hydrogen demand.

Regarding the buffer sizing, as shown in the following figure, unmet demand, expressed as percentage of the initial request, cannot be eliminated with increasing sizes, and further reductions become marginal compared to the significant increase in system size required. The buffer capacity was therefore set to a value equivalent to approximately two hours of hydrogen refueling demand.

Buffer cost analysis results

Storage size	1.02	tons
Pressure	31	bar
Storage cost	0.51	М€
Installation costs	28	%
Indirect costs	36	%
CAPEX	0.89	M€

Table 5.14: Buffer cost analysis results

To decide the storage configuration, and subsequently the size, the storage performance was evaluated in each configuration, through the unmet demand parameter, or miss-

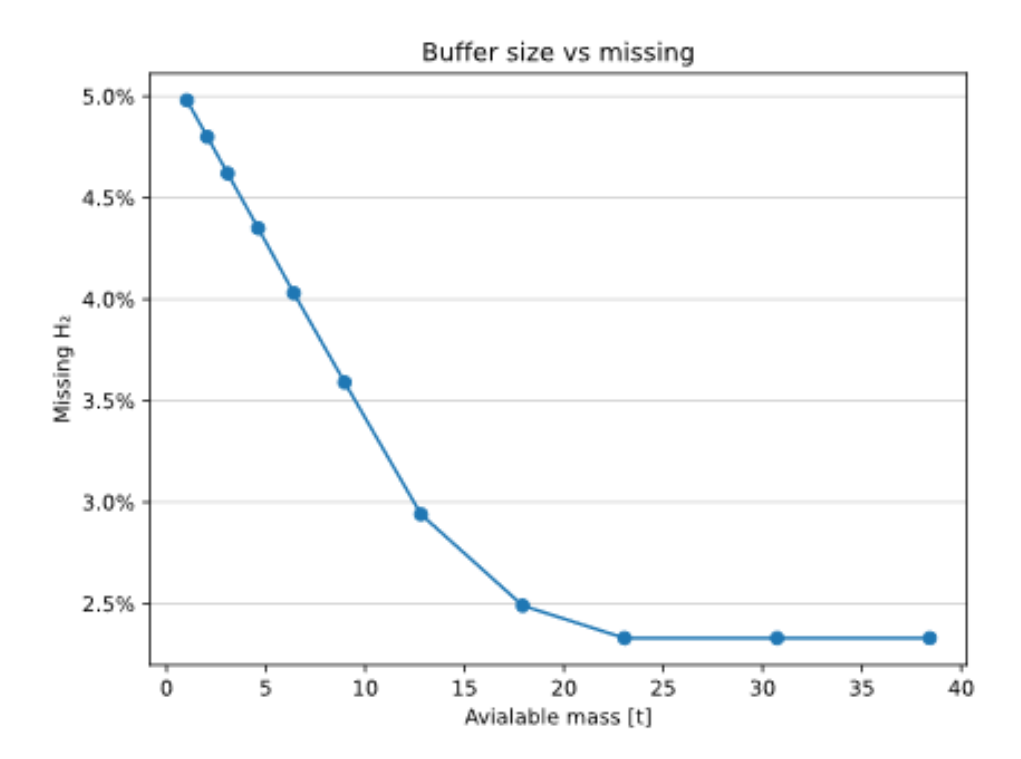


Figure 5.5: Buffer size versus missing

ing. Two storage configurations were considered: HP-only and MP-HP, as described in Section 4.4.

The following graphs show the unmet demand as a function of the storage size, for both the HP-only configuration and the combined MP-HP configuration. It can be observed that, for the same overall storage size, the HP-only setup results in a lower percentage of unmet demand. For this reason, the HP-only configuration was selected.

Furthermore, it can be observed that, with the power generation capacity kept constant, it is not possible to fully meet the consumption without requiring a significant increase in storage size.

The HP storage size was defined based on the slope of the curve. In the left part of the curve, the slope is steeper, indicating that a significant reduction in unmet demand can be achieved with relatively small increases in storage volume. By analyzing different HP storage capacities with respect to the resulting LCOH, the final storage size was chosen to keep the unmet demand below 5% and the LCOH below $10 \in /kg$.

Based on the consideration outlined in the previous section, the plant was dimensioned,

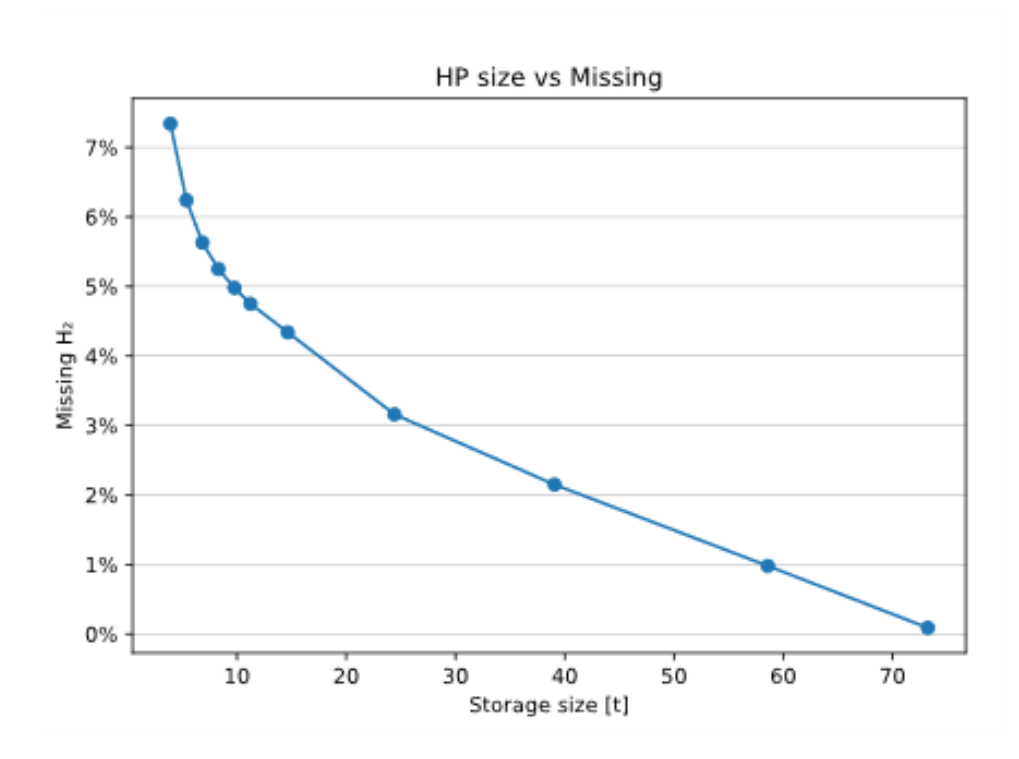


Figure 5.6: HP storage size versus missing

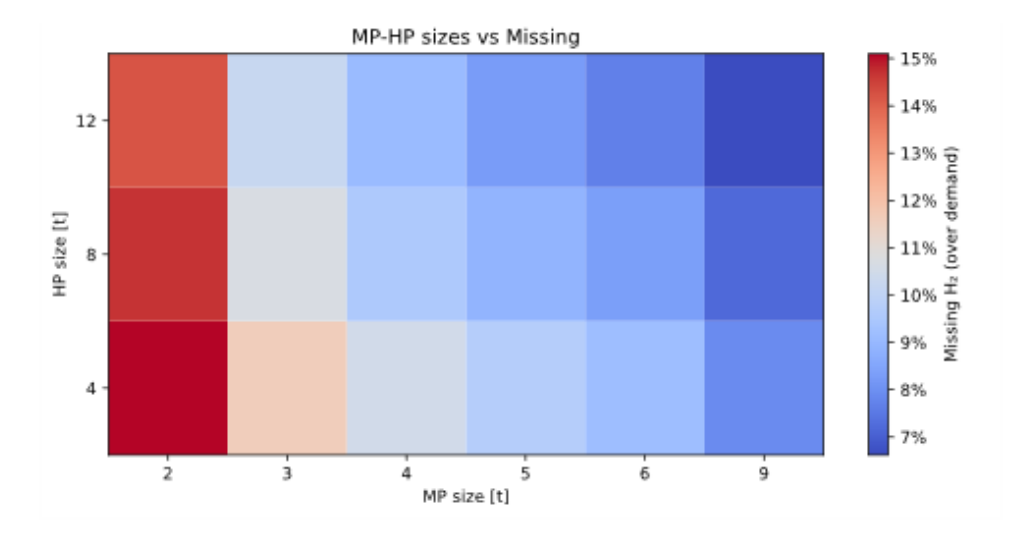


Figure 5.7: MP-HP storage size combinations versus missing

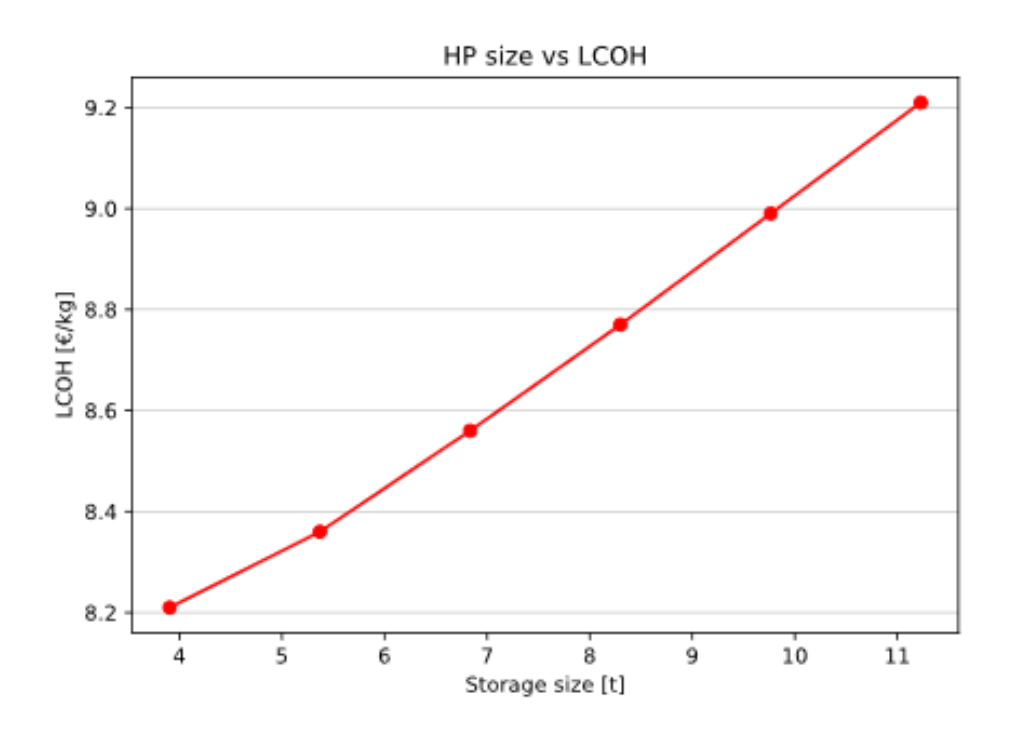


Figure 5.8: HP storage size versus LCOH

leading to the following results.

Base-case	\mathbf{p}	lant	d	lesign
	г.		_	

WIND farm	29	MW
Battery	11	MW
Electrolyzer	7	MW
Buffer (31 bar)	1.02	tons
HP storage (951 bar)	9.76	tons
Unmet demand	4.98	%
H ₂ annual consumption	844.2	tons

Table 5.15: Base-case plant design

From the model's results, the compressor cost analysis results were derived and the LCOE, LCOH and cost of hydrogen.

Compressor cost analysis results

Compression power	1986	kW
Specific power	7148	kW/kg/s
Compressor cost	2.14	M€
Specific cost	1079	€/kW
Compressor consumption	1.26	GWh/y
Compressor operating cost (electricity)	0.29	M€
Opex	0.13	M€
Installation costs	28	%
Indirect costs	36	%
CAPEX	3.73	M€

Table 5.16: Compressor cost analysis results

Economic key performance indicators

LCOE	40.73	€/MWh
LCOH	8.99	€/kg
H_2 energy cost	269.63	€/MWh
CAPEX-overall	88.03	M€

Table 5.17: Economic key performance indicators

5.4 Base-case design discussion

The behavior of the model's components was analyzed over the entire reference year of operation in order to assess the robustness of the design. Starting from the power farm, the resulting energy production was evaluated, highlighting the strong variability of the wind resource.

The Figure 5.10 illustrates the state of charge of the buffer over time. A variable trend can

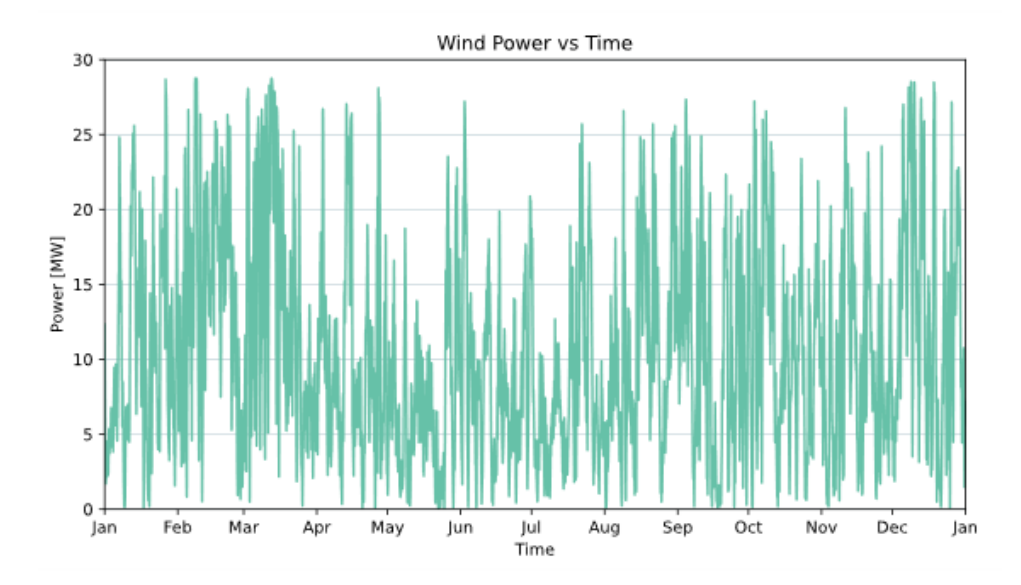


Figure 5.9: Wind energy production

be observed, with the minimum values corresponding to the amount of hydrogen required to maintain the minimum pressure of 7.9 bar. The buffer acts as a temporary storage unit, facilitating the transfer of hydrogen to the subsequent storage systems. The results show that the buffer fulfills this role, as its state of charge remains at low levels for most of the time, indicating the continuous transfer of hydrogen downstream. However, several peak periods are also evident. The most significant ones occur in February-March, coinciding with high wind power generation and therefore increased electrolyzer operation, and in August-December, which correspond to modeled periods when the truck fleet is not in use.

These same periods also exhibit the highest levels of hydrogen curtailment (Figure 5.11), driven by the combination of elevated renewable production and reduced demand. The HP storage follows the same trend (Figure 5.12).

The main findings from the sizing analysis can be summarized as follows:

- 1. Under the given conditions, the hydrogen demand cannot be fully met due to the high variability of renewable resources. Wind generation exhibits a variable trend, with long periods of underproduction and important peaks.
- 2. The key parameter influencing the system sizing is power generation. With a fixed

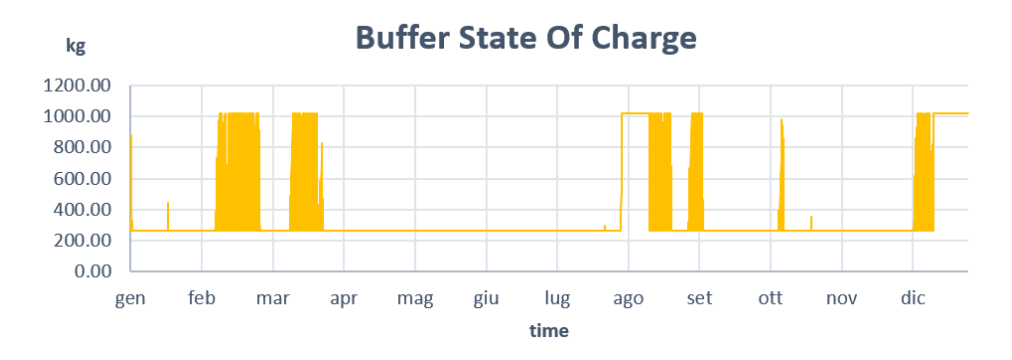


Figure 5.10: Buffer state of charge

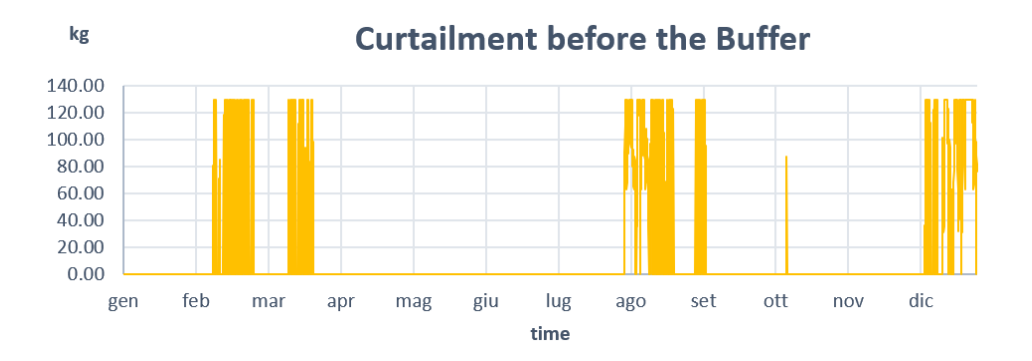


Figure 5.11: Buffer curtailment

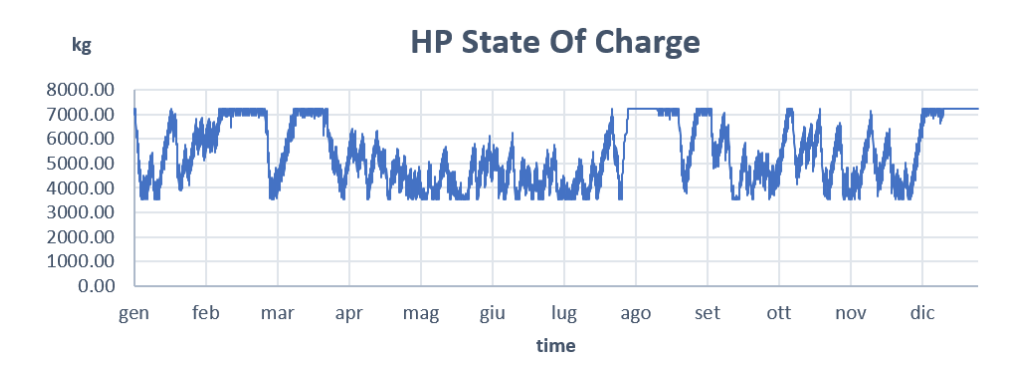


Figure 5.12: High pressure storage state of charge

wind capacity, meeting the demand would require extremely large storage volumes, indicating that storage alone is insufficient to fully compensate for wind variability.

3. During periods of zero consumption, especially when these extend over several consecutive weeks, it is more efficient to shut down the electrolyzer and suspend hydrogen production, thereby avoiding the need to vent the gas.

Although the system is fully supplied by renewable energy, there are certain hours (22 h/y) in which it exceeds the permitted emission threshold and, therefore, cannot be classified as renewable. This occurs mainly in two situations. First, the compressors, which are powered exclusively by the grid, may consume more energy for hydrogen compression than the amount of hydrogen produced, since production during those hours is very low and consequently the emission benchmark is also low. Second, when the electrolyzer is in standby mode: in these cases, the available renewable generation is insufficient for hydrogen production, and the battery contribution is also inadequate. At the same time, there is not enough energy to maintain the electrolyzer in standby, resulting in additional grid consumption and, consequently, associated emissions.

6 Sensitivity analysis

The sensitivity analysis was performed in two consecutive steps.

In the first step, many plant configurations were evaluated by varying battery size, grid connection and renewable energy mix. For each configuration, the main KPIs, such as LCOH, unmet demand, annual hydrogen production and CAPEX were calculated. This allowed the identification of the optimal investment, the configuration that represents the best trade-off between technical performance and cost.

In the second step, the selected optimal configuration was scaled to meet the case-study hydrogen demand, ensuring that the system could satisfy consumption requirements while maintaining the economic performance achieved in the first step.

6.1 Optimal investment

The optimal investment evaluation was conducted by collecting data from various plant configurations and representing them in a scatter plot. This approach was selected in order to understand which configurations represent the most profitable investments. Within the scatter plot, a Pareto front was identified. The Pareto front, a concept from multi-objective optimization, represents the set of solutions for which no objective can be improved without compromising another. In the context of a scatter plot, the Pareto front highlights the trade-offs between competing objectives, LCOH and H₂ net production in this case, allowing for the identification of the most efficient or "non-dominated" solutions.

All configurations were evaluated while keeping the storage capacity fixed at the basecase level, aiming to maximize production efficiency. This approach was chosen due to base-case design results indicating that renewable power farm is the most influencing parameter in the design. The aim is to find the point where is best to scale the storage, with the additional increase in renewable capacity being not otpimal anymore.

For a hydrogen production plant model, several configurations can be considered to perform a comprehensive sensitivity analysis:

1. Presence/absence of electricity storage systems

With battery \rightarrow allows storing excess renewable electricity and optimizing electrolyzer operation.

Without battery \rightarrow production is directly linked to the availability of renewable energy.

2. Grid connection

With grid \rightarrow enables the integration of grid electricity to increase production or stabilize the plant.

Without grid \rightarrow fully off-grid plant, dependent only on dedicated renewable sources.

3. Renewable energy mix

Wind only \rightarrow production based exclusively on wind turbines.

Wind and solar \rightarrow a hybrid configuration combining wind and photovoltaic sources helps reduce variability and improve overall energy availability. In this case, the solar contribution was reintroduced because the analysis considers the system as a whole, aiming to highlight the potential benefits of including PV generation.

Different installed capacities \rightarrow varying total installed capacities of wind and solar to find the best combination for net production.

The optimal configurations in the Pareto front were further filtered based on CAPEX (Figure 6.2,).

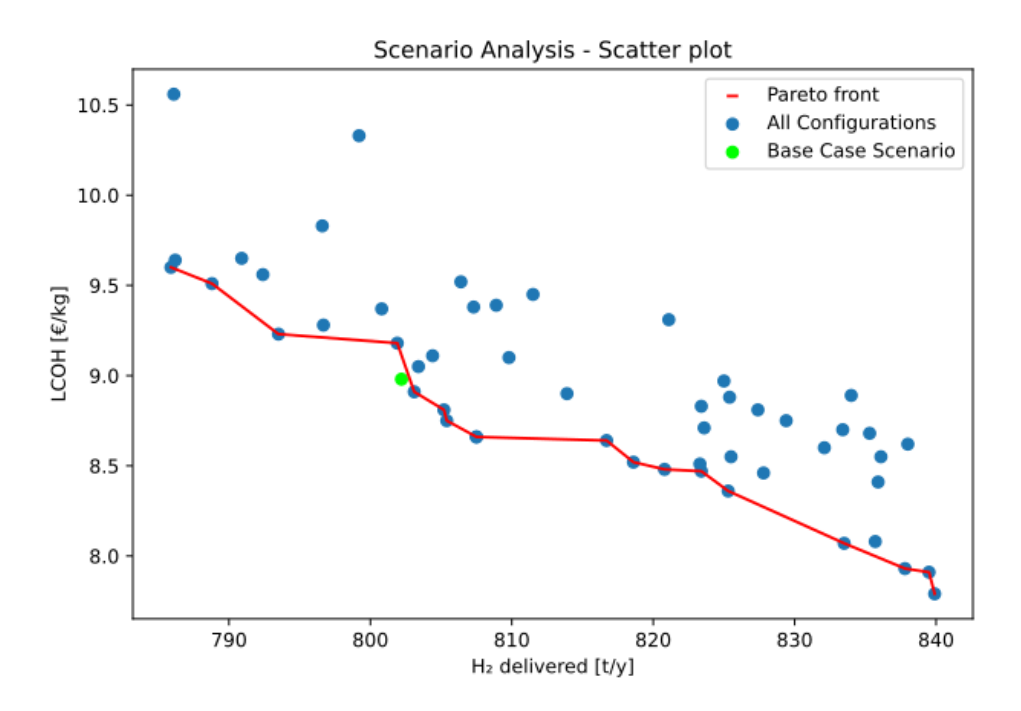


Figure 6.1: Scatter plot on different configurations

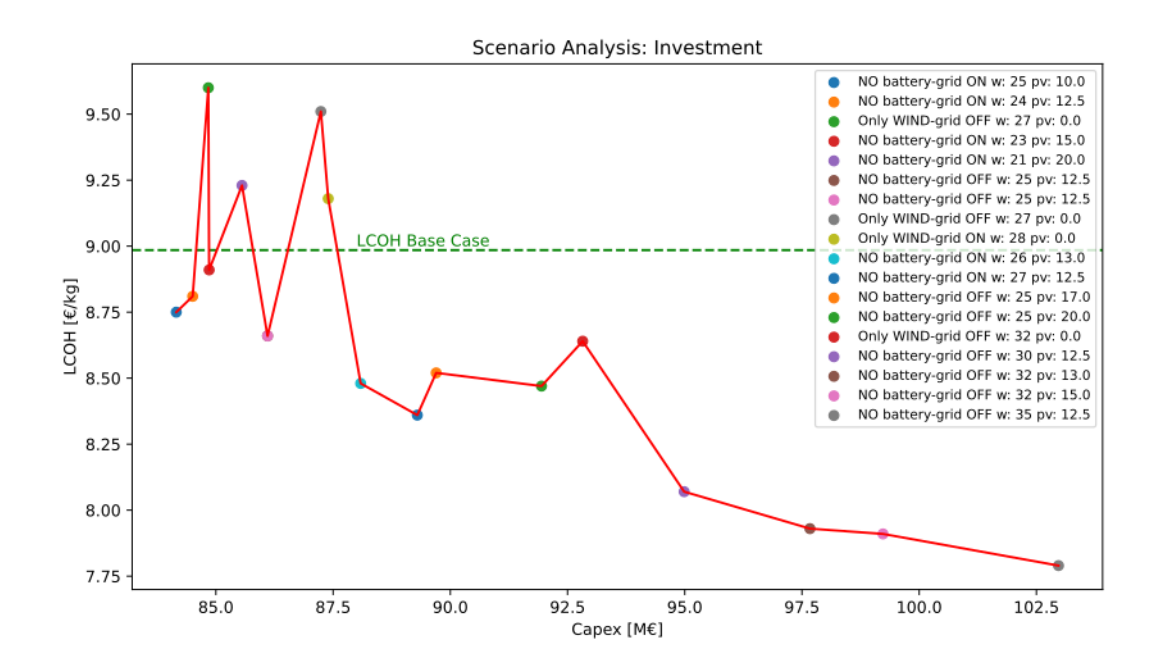


Figure 6.2: LCOH by CAPEX

The reference LCOH corresponded to the base-case scenario, and only those configurations with values below this threshold were considered. The configurations corresponding to local peaks in the curve were discarded. Between the remaining points, linearization was carried out (Figure 6.3,).

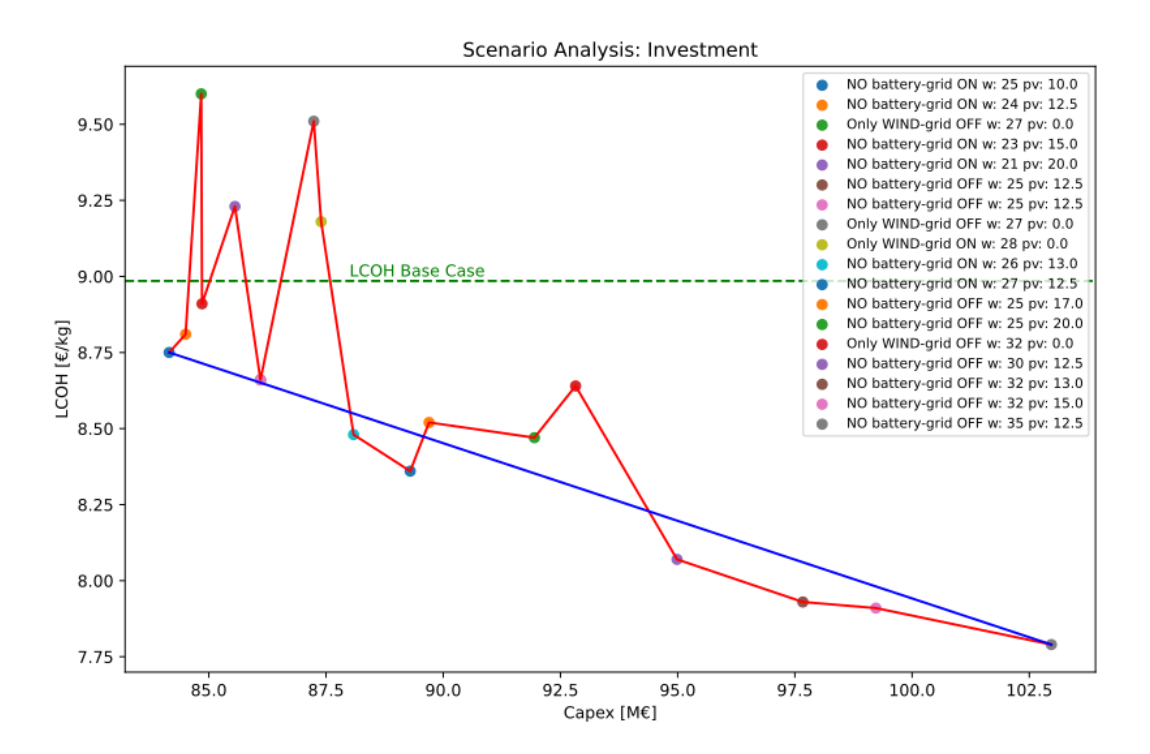


Figure 6.3: LCOH by CAPEX

All the points above the line were discarded. Furthermore, the configuration NO battery-grid OFF w:32 pv:15 (pink point) shows an almost zero slope, and thus no significant reduction in LCOH, compared to the adjacent configuration and so it was also discarded. In Figure 6.4 are shown the selected configurations.

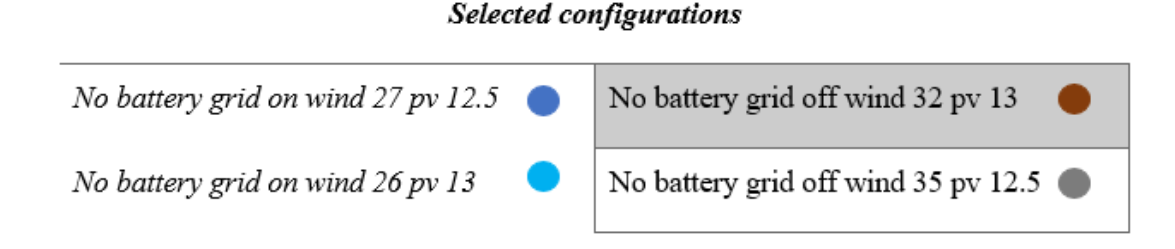


Figure 6.4: Selected configurations

The selected configurations are all designed without battery storage. This outcome represents a significant result, as it highlights that the contribution of the battery is not critical

in ensuring the hourly energy balance of the system. In fact, the stabilizing effect that a battery could provide is effectively compensated by the integration of photovoltaic capacity, which helps to mitigate variability and improve overall system reliability. This finding suggests that, under the given assumptions, investments in battery storage may not be justified from a techno-economic perspective, as their role can be effectively replaced by an optimized PV generation.

The behavior of the key parameters, namely: the LCOH, the CAPEX, the net H_2 delivered, the LCOE and the percentage of hours in which the system can be considered renewable, across the four selected configurations is clearly illustrated by a spider (radar) chart (Figure 6.5).

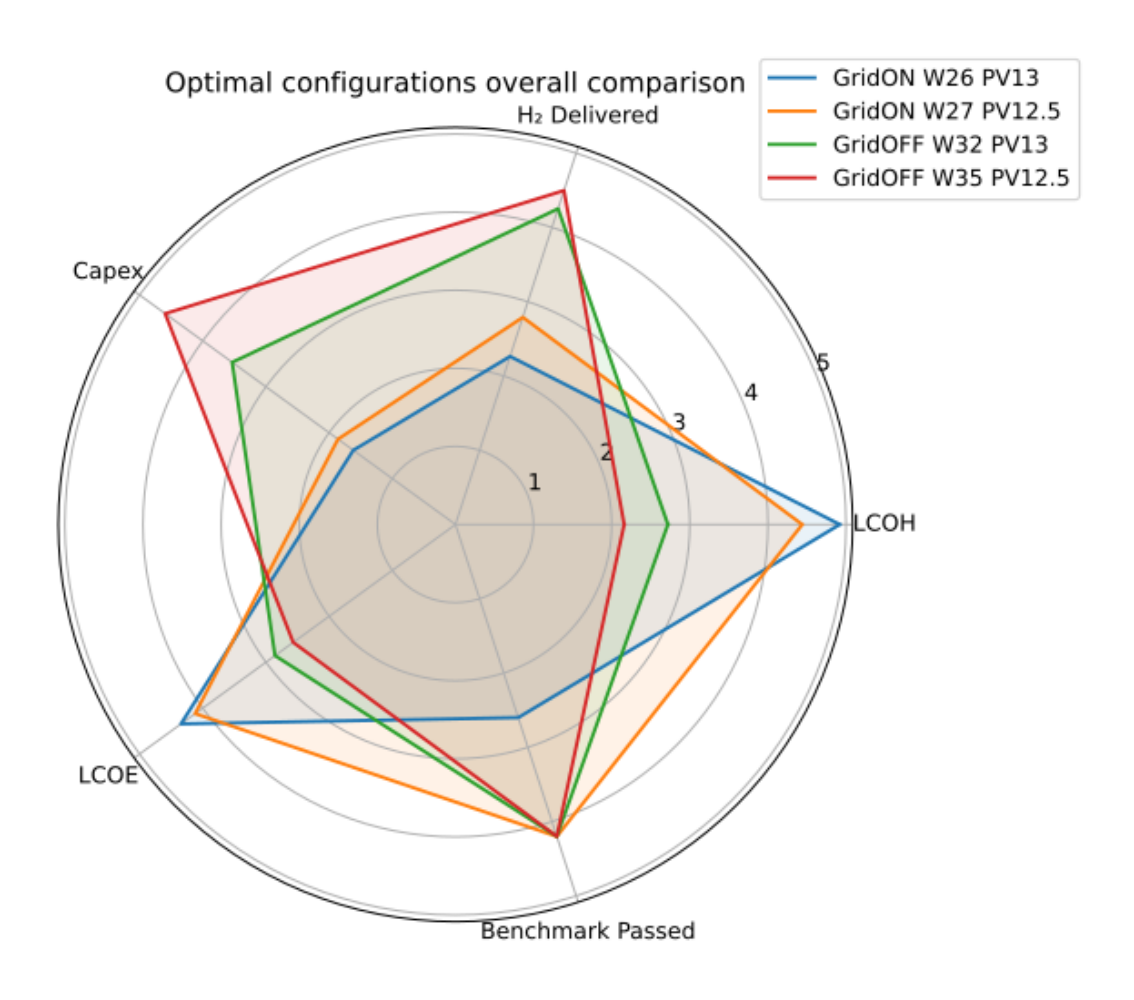


Figure 6.5: Optimal configuration comparison

The selected configurations can be regarded as optimal investment options. The grid-on configurations have higher LCOH and LCOE due to grid cost being higher than renewable

electricity, lower net H₂ delivered and less renewable hours in the year, but present lower CAPEX. Conversely, the two off-grid configurations achieve significantly higher production volumes, which leads to a considerable reduction in the LCOH. Although these options imply greater upfront investment, their enhanced production efficiency improves overall economic performance, making them competitive in the long term.

Optimal design	1	2	3	4
Wind Farm [MW]	26	27	32	35
Solar PV [MW]	13	12.5	13	12.5
Electrolyzer [MW]	7	7	7	7
Buffer (31 bar)	$400m^3(1.02t)$	$400m^3(1.02t)$	$400m^3(1.02t)$	$400m^3(1.02t)$
HP storage (951 bar)	$199.5m^3(9.76t)$	$199.5m^3(9.76t)$	$199.5m^3(9.76t)$	$199.5m^3(9.76t)$
Grid connection	YES	YES	NO	NO
Unmet demand	2.77%	2.24%	0.75%	0.51%
LCOH [€/kg]	8.48	8.36	7.93	7.79
CAPEX [M€]	88.09	89.30	97.67	102.07

Table 6.1: Optimal configurations

6.2 Optimal design

In the zero missing design, once this optimal configuration was selected, the buffer and storage capacity was subsequently scaled to match the actual hydrogen demand, ensuring that the system could meet consumption requirements while maintaining the previously determined economic performance.

From these analyses, it emerges that the first two configurations reach the target hydrogen demand only gradually, meaning that a significant scaling of the HP storage would be required. Such an increase, however, would not be economically convenient, as the last two configurations achieve better techno-economic performance. On the other hand,

increasing the buffer capacity leads to an asymptotic trend in hydrogen production, confirming that it is not sufficient on its own to fully match the demand.

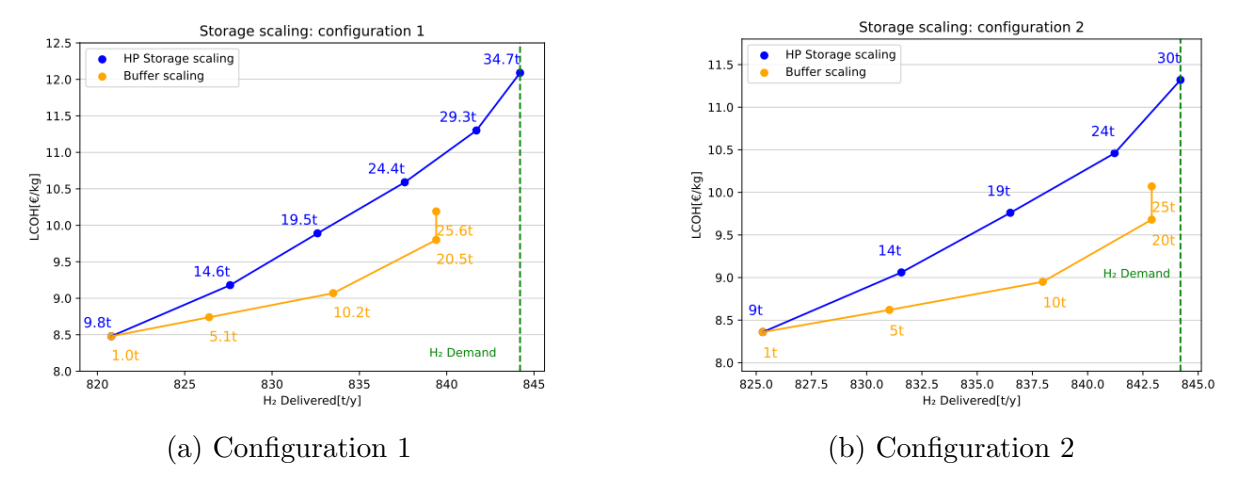


Figure 6.6: Grid ON Configurations

The last two configurations therefore represent the most economically viable solutions for achieving the desired production level. Increasing the buffer capacity proves to be consistently less expensive than scaling up the HP storage; and although the required buffer volumes are relatively large, their impact on both CAPEX and LCOH remains considerably lower.

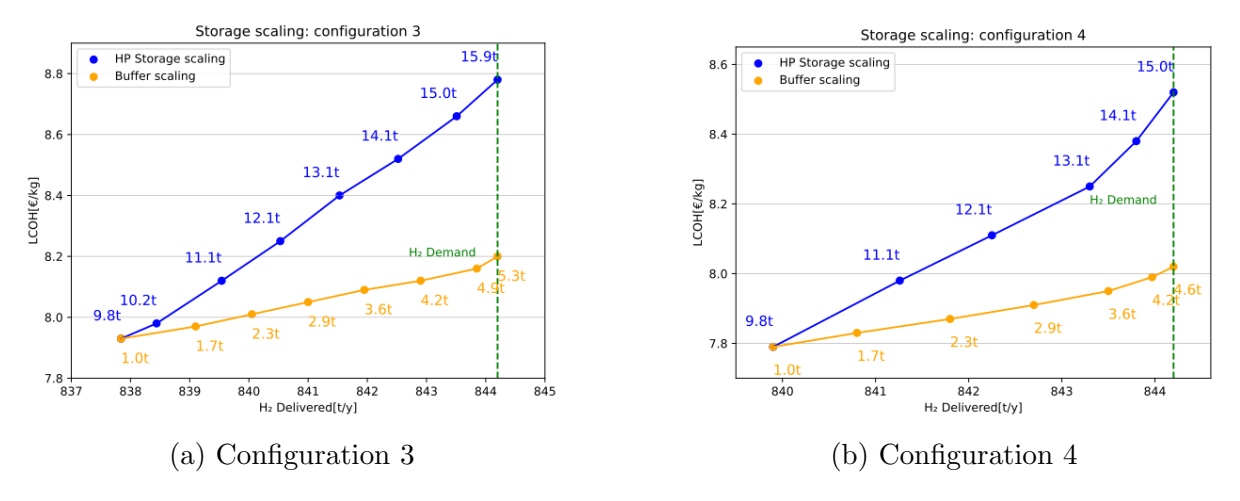


Figure 6.7: Grid OFF Configurations

The overall results are:

These configurations represent an optimal investment for achieving the required hydrogen fuel production. However, a drawback arises from the fact that, in the current model, the compressor of the hydrogen refueling station is connected exclusively to the grid.

Optimal design	Conf. 3	Conf. 4
Wind Farm [MW]	32	35
Solar PV [MW]	13	12.5
Electrolyzer [MW]	7	7
Buffer (31 bar)	$2050m^3(5.25t)$	$1800m^3(4.61t)$
HP storage (951 bar)	$199.5m^3(9.76t)$	$199.5m^3(9.76t)$
Grid connection	NO	NO

Table 6.2: Overall results (buffer scaling)

KPI	Conf. 3	Conf. 4
Net H ₂ delivered [t]	844.2	844.2
LCOH [€/kg]	8.19	8.02
CAPEX [M€]	101.35	105.19
Benchmark fails [h]	198	231

Table 6.3: key performance indicators (buffer scaling)

Consequently, increasing the buffer capacity leads to a higher number of operating hours in which the system cannot be considered fully renewable. This is represented by the Benchmark fails parameter in the previous table. This occurs because, during periods without renewable electricity generation and when the HP storage is depleted, hydrogen is supplied from the buffer, requiring compression up to the vehicle delivery pressure using grid electricity.

To address this issue, despite its lower economic convenience, it becomes necessary to scale up the HP storage. In this configuration, the hydrogen required for refueling can be supplied through pressure equalization, while compression takes place during periods of renewable electricity availability, thus preserving the renewable character of the system.

Optimal design	Conf. 3	Conf. 4
Wind Farm [MW]	32	35
Solar PV [MW]	13	12.5
Electrolyzer [MW]	7	7
Buffer (31 bar)	$400m^3(1.02t)$	$400m^3(1.02t)$
HP storage (951 bar)	$325.2m^3(15.92t)$	$307m^3(15.04t)$
Grid connection	NO	NO

Table 6.4: Overall results (HP scaling)

KPI	Conf. 3	Conf. 4
Net H ₂ delivered [t]	844.2	844.2
LCOH [€/kg]	8.78	8.52
CAPEX [M€]	108.38	111.25
Benchmark fails [h]	32	39

Table 6.5: key performance indicators (HP scaling) $\,$

7 Future work

For what concerns the use of hydrogen in the production process, a more immediate implementation, both in terms of costs and retrofit possibilities, involves the use of the UTIS patent for the introduction of a very small percentage of hydrogen into furnaces. This approach is applicable to general combustion systems, not limited to the cement sector, and does not aim to replace the existing fuel, but rather to improve combustion efficiency. When applied in continuous combustion systems, this method leads to an increase in furnace wall temperatures and re-ignition, thereby reducing fuel consumption and achieving more complete and optimized combustion. As a result, certain types of pollutants produced by incomplete combustion or other secondary processes are also reduced.

The radicals generated by the injection of trace amounts of H_2 (0.0001% to 0.01% v/v) accelerate the oxidation of unburned compounds. Consequently, the flame becomes more stable, and the production of CO, VOCs, particulate matter, and NO_X is reduced. At the same achieved temperature, fuel throughput can be decreased by approximately 5-7%, although this value is case-dependent. Hydrogen is injected along the furnace chamber at locations where the thermal profile allows immediate auto-ignition (zones with incandescent particles).

The injection can be performed continuously, which is more effective for NOx reduction, or in a pulsed manner, which is more favorable for the mitigation of CO and VOCs. The injection pressure must exceed the pressure within the combustion chamber and can be regulated through valves (rotary valves in the case of pulsed injection). Injection control is

implemented via a cascade logic system, which monitors key parameters (VOC/CO) and modulates hydrogen dosing to prevent accumulation and ensure complete combustion.

Another relevant design concept to investigate, in the context of hydrogen utilization in the production process, involves the partial substitution of 9% of the kiln fuel with hydrogen, in line with the European Net Zero vision for 2050 [42]. This target represents the goal to be achieved in the coming years and entails significant modifications to combustion dynamics and flame stability. Analyzing the potential impacts of this substitution constitutes an important step toward understanding and facilitating the practical implementation of hydrogen in industrial combustion processes.

Regarding the introduction of CCS and CCU technologies, a more comprehensive analysis is required to fully understand their potential. In particular, it is essential to investigate the possible future markets opportunities to commercialize the chemicals and the regulatory framework that can highlight their renewable origin and allow the diffusion. Additionally, all the supply chain linked to the transport of CO₂ to the conversion plants and consequential logistic of e-fuel distribution needs to be figured out. Such a study would provide a clearer picture of the practical opportunities and challenges related to integrating CCUS technologies into cement industrial process and could guide strategic decisions for both technological implementation and market development.

8 Conclusion

This master's thesis aims to assess the feasibility of renewable hydrogen for an industrial application. In particular, the work focuses on its potential implementation for the decarbonization of the transport fleet of an Irish cement production plant. This option was selected after evaluating and excluding other possible hydrogen integration pathways, such as its direct use in the production process or in CCU for the synthesis of e-fuels.

The analysis begins with a detailed assessment of the plant's production and energy consumption data, in order to establish the baseline hydrogen demand and to determine the nominal capacity of the electrolyzer. Subsequently, a hydrogen production plant model was developed in Excel, and partially implemented in Python to enable further improvements and dynamic analysis. The model includes several system components: an electrolyzer, a renewable power farm composed of photovoltaic systems and wind turbines, a battery storage system, a buffer tank, and a high-pressure storage unit designed to supply hydrogen to vehicles via pressure equalization (cascade refueling).

Following the implementation of the model, an economic assessment was carried out, including a cost analysis of the main components, with the aim of estimating specific costs.

A base-case configuration was developed using an incremental analysis approach, where each system component was sized individually while keeping the others fixed and the main economic indicators such as LCOH, LCOE, overall capex and opex were identified, along with capex breakdown for each component.

The results of the base-case study highlighted that the primary driver for system dimen-

sioning is the available renewable power generation, whose variability represents the main challenge to ensuring continuous hydrogen supply to meet demand.

The key parameters of the resulting base-case design are summarized below.

Kev 1	parameters-base	case
-------	-----------------	------

Unmet demand	4.89	%
LCOE	40.73	€/MWh
LCOH	8.99	€/kg
H_2 energy cost	269.63	€/MWh
CAPEX-overall	88.03	M€

Table 8.1: Key parameters-base case

The analysis was further expanded through a sensitivity analysis, guided by the key findings from the base-case configuration and developed following a multi-objective simulation and optimization approach. Several plant configurations, mainly differing in renewable power generation capacity and composition, were simulated, and the results in terms of net hydrogen delivered and LCOH were plotted in a scatter chart. A Pareto front was identified, representing the configurations that provide the best trade-off between cost and performance.

These optimal configurations were further filtered based on CAPEX, selecting those for which a higher initial investment led to a lower hydrogen cost. The most promising configurations were then analyzed in detail and presented.

The results demonstrated that investing in a battery system is not justified from a technoeconomic perspective. The improvement in the overall energy balance is not adequately reflected in an hourly balance model, and the same stabilizing effect can be achieved through a properly sized photovoltaic farm. From this analysis, the PV system primarily enhances the stability of the power supply, while wind energy remains the main contributor to electricity generation. Moreover, although increasing the power farm capacity requires higher upfront investment, it significantly boosts hydrogen production and leads to a progressive reduction in the LCOH.

Finally, the scaling-up of both the buffer and the high-pressure storage was investigated, to reach a configuration able of meeting the total hydrogen demand. The storage sizing curves, expressed as storage volume versus hydrogen cost, show that investing in buffer scaling is more convenient than HP scaling. However, this approach increases the number of operating hours in which emissions exceed the allowed limit. This occurs because, during periods when the HP storage is depleted and renewable generation is insufficient, hydrogen is drawn from the buffer and must be compressed to delivery pressure. Since the compressor is connected to the electrical grid, this process leads to indirect emissions. As these conditions coincide with low renewable generation, the issue would persist even if the compressor were connected to the renewable generation.

Therefore, the final proposed design includes the scaling-up of the HP storage, despite its lower economic attractiveness, in order to ensure full compliance with emission limits. This configuration results in less than 40 hours per year in which emissions exceed the allowed threshold. The design successfully meets the hydrogen demand, achieving an LCOH between 8.52 and 8.78 €/kg, depending on the selected configuration among the two proposed.

Bibliography

- [1] International Energy Agency, "CO₂ Emissions in 2023," 2023. [Online]. Available: www.iea.org
- [2] International Energy Agency, "Global Hydrogen Review 2024," 2024. [Online]. Available: www.iea.org
- [3] Michael. Hirscher, Handbook of hydrogen storage: new materials for future energy storage. Wiley-VCH Verlag & Co., 2010.
- [4] T. Dell'idrogeno E Celle, C. I. M. Santarelli, and P. Di Torino, "Immagazzinamento di idrogeno come gas compresso."
- [5] G. AlZohbi, A. Almoaikel, and L. AlShuhail, "An overview on the technologies used to store hydrogen," Energy Reports, vol. 9, pp. 28-34, Oct. 2023, doi: 10.1016/j.egyr.2023.08.072.
- [6] N. Giovannini, "Analisi della regolazione a livello nazionale ed europeo sull'idrogeno: dal power-to-gas agli utilizzi finali," 2023.
- [7] "European Parliament and the Council of the European Union, 2023, Commission Delegated Regulation (EU) 2023/1184 of 10 February 2023 supplementing Directive (EU) 2018/2001 of the European Parliament and of the Council defining a Union methodology setting out detailed rules for the production of renewable liquid and gaseous transport fuels of non-biological origin. Official Journal of the European Union L 157/11, 20.6.2023.".

- [8] "European Parliament and the Council of the European Union, 2023, Commission Delegated Regulation (EU) 2023/1185 of 10 February 2023 supplementing Directive (EU) 2018/2001 of the European Parliament and of the Council by establishing a minimum threshold for greenhouse gas emissions savings of recycled carbon fuels and by specifying a methodology for assessing greenhouse gas emissions savings from renewable liquid and gaseous transport fuels of non-biological origin and from recycled carbon fuels. Official Journal of the European Union L 157/20, 20.6.2023.".
- [9] Hydroge valleys.
- [10] Sh2amrock Hydrogen Valley.
- [11] Aragon Hydrogen Foundation, "SH2AMROCK Sourcing Hydrogen for Alternative Mobility, Realising Opportunities and Creating Know How in Ireland.," Accessed 12/09/25.
- [12] "Energy Transition Commission, Sectoral Focus Cement, 2019."
- [13] International Energy Agency, "Technology Roadmap Low-Carbon Transition in the Cement Industry." [Online]. Available: www.wbcsdcement.org.
- [14] Mannok informations accessed 27/8/2025.
- [15] Mannok, Annual sustainability report 2020.
- [16] Wind Energy Market Intelligence-Wind Farms accessed 27/8/2025.
- [17] P. Mcdonagh, "Strategies to fully decarbonize cement production in Ireland," 2024. [Online]. Available: http://www.nuigalway.ie/engineering/
- [18] EPA, Annual Environmental Report Mannok Cement, 2024.
- [19] EMEP/EEA Air pollutant emission inventory guidebook.
- [20] I. Energy Agency, "Net Zero by 2050 A Roadmap for the Global Energy Sector," 2050. [Online]. Available: www.iea.org/t&c/

- [21] "Mannok, Annual sustainability report 2023".
- [22] Mannok, Sustainability strategy 2021-2030.
- [23] European Commission, Deep decarbonization of industry: the cement sector.
- [24] European Commission, 2021, Commission Implementing Decision (EU) 2021/1184 of 29 June 2021, Official Journal of the European Union.
- [25] F. Williams, A. Yang, and D. R. Nhuchhen, "Decarbonisation pathways of the cement production process via hydrogen and oxy-combustion," Energy Convers Manag, vol. 300, Jan. 2024, doi: 10.1016/j.enconman.2023.117931.
- [26] L. Desport, C. Andrade, D. Corral, and S. Selosse, "Feasibility, conditions, and opportunities for achieving net-negative emissions in the global cement industry," International Journal of Greenhouse Gas Control, vol. 141, Feb. 2025, doi: 10.1016/j.ijggc.2024.104280.
- [27] M. D. Obrist, R. Kannan, T. J. Schmidt, and T. Kober, "Decarbonization pathways of the Swiss cement industry towards net zero emissions," J Clean Prod, vol. 288, Mar. 2021, doi: 10.1016/j.jclepro.2020.125413.
- [28] C. Kroumian, J. Maier, K. Peloriadi, G. Scheffknecht, and P. Grammelis, "Evaluation of 100% alternative fuel combustion under oxyfuel conditions in a pilot-scale burner for application in retrofit oxyfuel cement kiln," Fuel, vol. 381, Feb. 2025, doi: 10.1016/j.fuel.2024.133697.
- [29] G. Barigozzi, G. Brumana, G. Franchini, E. Ghirardi, and S. Ravelli, "Techno-economic assessment of green hydrogen production for steady supply to industrial users," Int J Hydrogen Energy, vol. 59, pp. 125–135, Mar. 2024, doi: 10.1016/j.ijhydene.2024.02.033.
- [30] A. Ibáñez-Rioja et al., "Baseload hydrogen supply from an off-grid solar PV-wind power-battery-water electrolyzer plant," Energy, vol. 322, May 2025, doi: 10.1016/j.energy.2025.135304.

- [31] L. Pilotti, A. F. Castelli, and E. Martelli, "Optimal design of fully renewable and dispatchable power plants with hydrogen seasonal storage," Renew Energy, vol. 241, Mar. 2025, doi: 10.1016/j.renene.2024.122195.
- [32] K. Kunasegeran, A. A. A. Raman, U. J. Alengaram, and A. Buthiyappan, "Greener Cement Production Through In-Situ Carbon Capture and Utilization: A Review," Chemical Engineering and Processing - Process Intensification, p. 110468, Nov. 2025, doi: 10.1016/j.cep.2025.110468.
- [33] S. Barbhuiya, B. Bhusan Das, and D. Adak, "Roadmap to a net-zero carbon cement sector: Strategies, innovations and policy imperatives," May 01, 2024, Academic Press. doi: 10.1016/j.jenvman.2024.121052.
- [34] A. Rafiq, J. Ren, N. Laosiripojana, T. Silalertruksa, and S. H. Gheewala, "Life cycle environmental and economic viability analysis of CO₂ utilization for chemical production in the cement sector," Sustain Prod Consum, vol. 58, pp. 364–384, Sep. 2025, doi: 10.1016/j.spc.2025.06.011.
- [35] M. Genovese and P. Fragiacomo, "Hydrogen refueling station: Overview of the technological status and research enhancement," May 01, 2023, Elsevier Ltd. doi: 10.1016/j.est.2023.106758.
- [36] T. A. Gunawan and R. F. D. Monaghan, "Techno-econo-environmental comparisons of zero- and low-emission heavy-duty trucks," Appl Energy, vol. 308, Feb. 2022, doi: 10.1016/j.apenergy.2021.118327.
- [37] J. Kast, G. Morrison, J. J. Gangloff, R. Vijayagopal, and J. Marcinkoski, "Designing hydrogen fuel cell electric trucks in a diverse medium and heavy duty market," Research in Transportation Economics, vol. 70, pp. 139–147, Oct. 2018, doi: 10.1016/j.retrec.2017.07.006.
- [38] M. Martorelli, M. Genovese, and P. Fragiacomo, "Enhancing heavy duty vehicle hydrogen refueling by alternative approach to SAE J2601/2 protocol and

- flow dynamics," Int J Hydrogen Energy, vol. 101, pp. 234–249, Feb. 2025, doi: 10.1016/j.ijhydene.2024.12.378.
- [39] R. A. Öztürk and Y. Devrim, "Optimal design and technoeconomic analysis of onsite hydrogen refueling station powered by wind and solar photovoltaic hybrid energy systems," Renew Energy, vol. 245, Jun. 2025, doi: 10.1016/j.renene.2025.122788.
- [40] W. Zieri and I. Ismail, "Alternative Fuels from Waste Products in Cement Industry," in Handbook of Ecomaterials, Springer International Publishing, 2018, pp. 1-24. doi: 10.1007/978-3-319-48281-1_142-1.
- [41] A. S. Ansar, A. S. Gago, F. Razmjooei, R. Reißner, Z. Xu, and K. A. Friedrich, "Al-kaline electrolysis—status and prospects," in Electrochemical Power Sources: Fundamentals, Systems, and Applications Hydrogen Production by Water Electrolysis, Elsevier, 2021, pp. 165–198. doi: 10.1016/B978-0-12-819424-9.00004-5.
- [42] I. Energy Agency, "Net Zero Roadmap: A Global Pathway to Keep the 1.5 °C Goal in Reach 2023 Update," 2023. [Online]. Available: www.iea.org/t&c/
- [43] European Union, "European Hydrogen Observatory, Electrolyzer Cost, Accessed 18/09/2025.
- [44] S. Krishnan et al., "Present and future cost of alkaline and PEM electrolyser stacks," Int J Hydrogen Energy, vol. 48, no. 83, pp. 32313–32330, Oct. 2023, doi: 10.1016/j.ijhydene.2023.05.031.
- [45] European Commission, 2021, Commission Implementing Decision (EU) 2021/1184 of 29 June 2021, Official Journal of the European Union.
- [46] International Energy Agency, IEA- Transport, Accessed 18/09/2025.
- [47] International Energy Agency, CO₂ Emissions in 2022.
- [48] O. Delgado et al., "Fuel efficiency Technology in european heavy-Duty vehicles: Baseline and potential For The 2020-2030 Time Frame," 2017. [Online]. Available: www.theicct.org

BIBLIOGRAPHY

- [49] H. Basma and F. Rodríguez, "Fuel cell electric tractor-trailers: Technology overview and fuel economy," 2022. [Online]. Available: www.theicct.org
- [50] European Commission, Delegated Regulation, Directive (EU) 2023/1185, 10 February 2023, Official Journal of the European Union.
- [51] "Covenant of Mayors for Climate and Energy: Greenhouse gas emission factors for local emission inventories," doi: 10.2760/521074.
- [52] I. Renewable Energy Agency, Renewable power generation costs in 2024. [Online].

 Available: www.irena.org
- [53] A. A. Kebede et al., "Techno-economic analysis of lithium-ion and lead-acid batteries in stationary energy storage application," J Energy Storage, vol. 40, Aug. 2021, doi: 10.1016/j.est.2021.102748.
- [54] P. Marocco, D. Ferrero, A. Lanzini, and M. Santarelli, "Optimal design of standalone solutions based on RES + hydrogen storage feeding off-grid communities," Energy Convers Manag, vol. 238, Jun. 2021, doi: 10.1016/j.enconman.2021.114147.
- [55] I. Renewable Energy Agency, Making the breakthrough: Green hydrogen policies and technology costs. 2021. [Online]. Available: www.irena.org
- [56] Technology Data-Energy storagetechnologydata Design and production: Danish Energy Agency.
- [57] G. Parks, "Hydrogen Station Compression, Storage, and Dispensing Technical Status and Costs: Systems Integration," 2020, doi: 10.13140/RG.2.2.23768.34562.
- [58] I. Renewable Energy Agency, IRENA Resource Data Methodology.
- [59] V. Anatolitis et al., The cost of financing for renewable power. 2023. [Online]. Available: www.irena.org
- [60] Sustainable Energy Authority Ireland, "SEAI statistics: prices," Accessed 18/09/2025 https://www.seai.ie/data-and-insights/seai-statistics/prices.

[61] T. A. Gunawan, A. Singlitico, P. Blount, J. Burchill, J. G. Carton, and R. F. D. Monaghan, "At what cost can renewable hydrogen offset fossil fuel use in Ireland's gas network?," Energies (Basel), vol. 13, no. 7, Apr. 2020, doi: 10.3390/en13071798.